



ELSEVIER

Contents lists available at ScienceDirect

# Quaternary Science Reviews

journal homepage: [www.elsevier.com/locate/quascirev](http://www.elsevier.com/locate/quascirev)

## A post-glacial relative sea level curve for the central Douglas Channel area, British Columbia, Canada

Bryn Letham <sup>a,\*</sup>, Dana Lepofsky <sup>a</sup>, Spencer Greening <sup>a,b</sup><sup>a</sup> Simon Fraser University Department of Archaeology, Canada<sup>b</sup> Gitga'at Oceans and Lands Department, Canada

## ARTICLE INFO

## Article history:

Received 19 August 2020

Received in revised form

26 April 2021

Accepted 9 May 2021

Available online 27 May 2021

Handling Editor: I Hendry

## Keywords:

Relative sea level change

Northwest coast

Douglas channel

Diatoms

Paleoshorelines

Terminal pleistocene

Deglaciation

Archaeology

Paleolandscape reconstruction

## ABSTRACT

We present a post-glacial relative sea level (RSL) curve for the Central Douglas Channel region on the northern Northwest Coast of North America spanning the last 14,500 years, constrained by 68 radiocarbon dated index and limiting points derived from multiple RSL proxies. We evaluate each proxy based on the reliability and specificity of the inference for indicating RSL position, allowing us to weight different methods of data collection. We determine that central Douglas Channel was ice-free following the Last Glacial Maximum by ~14,500 BP and RSL was at least 90 m higher than today. Isostatic rebound caused RSL to fall to 21 m asl by 11,500 BP, though there may have been a glacial re-advance that would have paused RSL fall around the beginning of the Younger Dryas. RSL fell to 10–15 m asl by 10,000 BP, and continued to drop at a slower rate towards its current position, which it reached by ~1800 years ago. This is the first well-constrained RSL reconstruction for a nearly 400 km stretch between the northern and central coasts of British Columbia, Canada. This reconstruction provides information about the timing and rate of deglaciation of western North America and exemplifies variability among sea level trends across the region. Long-term RSL reconstructions are integral to explorations of coastal change and archaeological inquiries into early coastal occupations.

© 2021 Elsevier Ltd. All rights reserved.

### 1. Introduction

Trajectories of post-glacial relative sea level (RSL) change vary significantly across the Northwest Coast of North America (Clague et al., 1982; Engelhart et al., 2015; Shugar et al., 2014), even over distances as little as tens of kilometers (Letham et al., 2016; McLaren et al., 2014). The causes of this variation include disparities in isostatic effects resulting from differences in the location and thickness of coast-adjacent ice sheets during the Wisconsin Glaciation and differences in the timing and rate of glacial retreat following the Last Glacial Maximum (LGM). Furthermore, variable tectonic uplift or subsidence and the localized effects of catastrophic events such as megathrust earthquakes (Mathewes and Clague, 1994; Hutchinson and Clague 2017) may also affect the relative position of sea level along the coast.

On coastlines as complex and varied as those of the Northwest

Coast, even relatively small changes in RSL can have dramatic impacts on the position of those coastlines and their associated environments. For Indigenous Peoples living on these coasts over the millennia, even subtle changes in RSL would have had an impact on their settlements and the ecosystems from which they derived their livelihoods. Reconstructing local RSL histories is a fundamental building block for understanding deep-time landscape history, and allows archaeologists and paleoecologists to model and understand these impacts (Letham et al., 2018; Mackie et al., 2018; McLaren et al., 2020). When coupled with Indigenous oral histories that recount coastal settlements being occupied as early as the coast was habitable, RSL reconstructions are a powerful tool for finding material evidence of the lives of these early occupants (e.g., Fedje and Mathewes, 2005; McLaren et al., 2015).

Given the dynamic long-term geomorphic histories along coasts and the fragmentary nature of the paleoenvironmental record, arguably the most robust way to reconstruct RSL change is by documenting multiple proxy measures that indicate directly or constrain the position of RSL from deglaciation to the present. RSL information can be gleaned from many types of sources, and it is

\* Corresponding author. Education Building 9635, 8888 University Dr., Burnaby, BC, V5A 1S6, Canada.

E-mail address: [bryn.letham@gmail.com](mailto:bryn.letham@gmail.com) (B. Letham).

now standard practice to build large datasets for RSL reconstruction (e.g., Khan et al., 2019; Shennan et al., 2015). Consideration must be given to landform stability and post-depositional processes that have impacted RSL proxies, but careful evaluation of large arrays of data can yield well-constrained, deep-time RSL reconstructions.

While there are several detailed RSL reconstructions for the Northwest Coast (e.g., Carlson and Baichtal, 2015; Clague et al., 1982; Fedje et al., 2005, 2018; Hutchinson et al., 2004a; James et al., 2005, 2009; Letham et al., 2016; McLaren et al., 2011, 2014; Roe et al., 2013), the central-north mainland coast of British Columbia remains a gap in our knowledge. Specifically, no RSL research has been conducted between Calvert Island/Hakai Pass on the central coast (McLaren et al., 2014) and the Prince Rupert area to the north (Fig. 1; Letham et al., 2016; see also Shugar et al., 2014). This region is important for coastal Indigenous history because it is in the middle of the coastal route over which the first human occupants of the continent may have traversed (Braje et al., 2019; Erlandson et al., 2007; Fladmark, 1979). Not surprisingly, this region is the homeland of many Indigenous groups with oral histories asserting very early coastal occupation and with rich archaeological records of coastal use and long-term habitation. This study addresses the spatial gap our understanding of Northwest Coast RSL histories and sets the stage for understanding the coastlines occupied by ancient peoples by presenting a RSL curve derived from multiple proxies for the central Douglas Channel area, 230 km north of Calvert Island, and 100 km south-southwest of Prince Rupert (Fig. 1).

### 1.1. Study area

We gathered data for RSL reconstruction in central Douglas Channel from the Kitkiata Inlet/Quaal River watershed, the

Kishkosh Inlet area, and valleys behind Hartley Bay (Fig. 1). Each are glacially carved watersheds that run west-northwest of Douglas Channel and join the channel at their mouths. Douglas Channel itself is a large glacial fjord connected to the Pacific Ocean and terminating at the city of Kitimat at the end of the Kitsumkalum-Kitimat Trough (Clague, 1984; MacDonald, 1983; Shaw et al., 2017). The region consists of coastal rainforest on the western flanks of the British Columbia Coast Mountains and is characterized by rugged and steep terrain; the valleys and inlets are surrounded by mountains that reach up to 1000 m asl. Shorelines in the area are generally steep and straight along inlet edges with interspersed pocket bays with creeks and sand or gravel beaches. At the heads of the inlets are large estuarine areas with extensive tidal flats. The area has a maximum tide range of 6.5 m, measured from a tide gauge at Hartley Bay (Table 1).

We gathered the bulk of our data from the meandering Quaal River and its terminus at Kitkiata Inlet. The area is strikingly low relief; at the lowest tides over 2.5 km of intertidal sand and mud flat is exposed southeast of the river mouth, and at the highest tides the river itself is tidally influenced up to 8.5 km up the valley. Even minor differences in RSL would have dramatically transformed these estuaries and river valleys. As expected of an active, meandering river, the riverbank is characterized by both long depositional sequences that document these landscape transformations, and slumped exposures of sediments containing indicators of these changes.

The study area is within the territory of Ts'msyen (anglicized as Tsimshian) peoples, who according to their worldview have lived here since time immemorial. Kitkiata Inlet is the core territory of a specific Ts'msyen tribe, the Gitk'a'ata, or Gitga'at (anglicized). The nearest town is the First Nations reservation in Hartley Bay at the south end of Douglas Channel (Fig. 1B), the primary settlement for

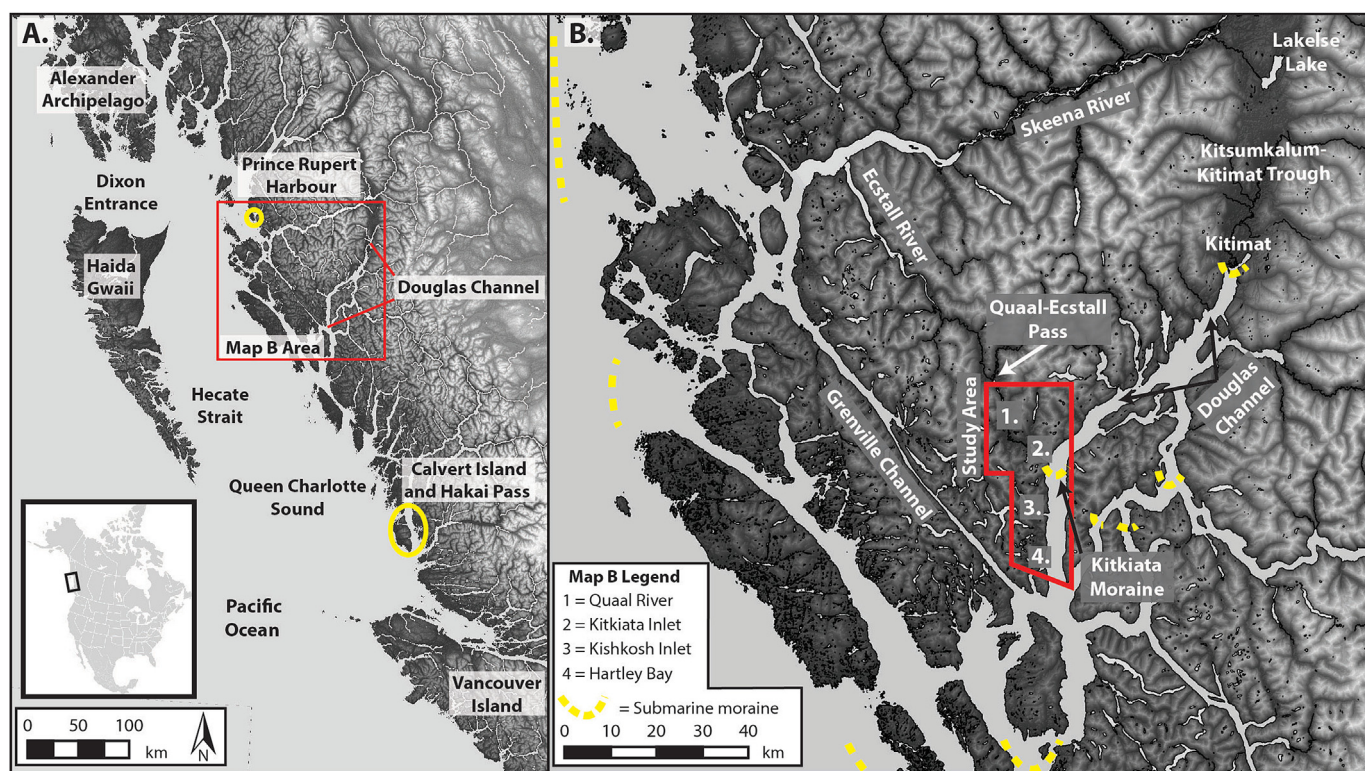


**Fig. 1.** A. Northwest Coast, indicating location of the Douglas Channel and locations mentioned in text. B. Douglas Channel area and Skeena River Valley, indicating study area and locations mentioned in the text. Yellow dashed lines indicate approximate locations of submarine moraines, derived from Bornhold (1983) and Shaw et al. (2017, 2020). The Kitkiata moraine discussed in text is indicated. (For interpretation of the references to colour in this figure legend, the reader is referred to the Web version of this article.)

**Table 1**

Tidal Parameters and their definitions for Canadian Hydrographic Survey Benchmark Station 9130 at Hartley Bay, predicted over 19 years, start year 2010 (Canadian Hydrographic Survey, personal communication, 2018).

Tidal Parameter	Abbreviation	Definition	Measurement above Chart Datum (m CD)	Equivalent elevation relative to geodetic mean sea level (m asl; used in this study)
Highest Astronomical Tide	HAT	Highest tide on an 18.6 year cycle.	6.271	3.35
Higher High Water Large Tide	HHWLT	The average of the highest high waters, one from each of 19 years of predictions.	6.184	3.263
Higher High Water Mean Tide	HHWMT	The average from all the higher high waters from 19 years of predictions.	5.138	2.217
High Water Mean Tide	HWMT	The average of the high water levels.	4.869	1.948
Mean Tide Level	MTL	The average of HWMT and LWMT.	3.188	0.267
Mean Sea Level	MSL	The average of all hourly water levels over the available period of record.	2.921	0
Lower Low Water Mean Tide	LLWMT	The average of all the lower low waters from 19 years of predictions.	1.058	-1.863
Lower Low Water Large Tide	LLWLT	The average of the lowest low waters, one from each of 19 years of predictions.	-0.049	-2.97
Lowest Astronomical Tide	LAT	Lowest tide on an 18.6 year cycle.	-0.179	-3.1

the Gitga'at today. Prior to European missionization and introduced diseases in the mid-1800s the Gitga'at lived throughout the Douglas Channel and surrounding areas in large settlements, harvesting and managing the resources of the land and sea. One such settlement is *Laxgalts'ap* ("Old Town"; Canadian archaeological site registry number FjTh-3), a Gitga'at reservation on the north shore of Kitkiata Inlet (Lepofsky et al., 2017; Marsden, 2012), where the archaeological record indicates human occupation extending back to the early Holocene. Additionally, oral traditions assert deep-time use of the watersheds. One Gitga'at lineage holds an *adawx* (oral history) that recounts their settling of the Kitkiata Inlet area long ago. This settlement was founded by a group of people who migrated up the Ecstall River (a tributary of the Skeena River to the north; Fig. 1B), over the low pass between the Ecstall watershed and the Quaal watershed, and down the Quaal River to Kitkiata Inlet (Marsden, 2012). Another Gitga'at *adawx* refers to a mountain refuge in the same watershed during a time of higher sea level/higher waters.

Linking these oral traditions to the realities of the early post-glacial landscape requires understanding how the position of the shoreline, the locations of ideal land for habitation, and passable travel corridors changed through time. RSL change since deglaciation would have been the primary driver of shoreline change. In the Quaal River Valley from mouth to head there is only a difference in elevation of about 15 m along a horizontal distance greater than 12 km, and half of that elevation gain (~7 m) occurs in the upper 2 km of the valley. Higher RSL through the end of the Pleistocene and the Holocene would have meant that Kitkiata Inlet would have extended much further up the valley, and the shorelines on which the founding Gitga'at populations settled would have been in different positions than those of today.

## 1.2. Glacial history

Douglas Channel is in the heart of a region with a complex glacial and post-glacial geomorphic history that was a prime driver of RSL change. After the Last Glacial Maximum (~27,000 to 18,000 years ago; Blaise et al., 1990; Clague et al., 2004:86) the Cordilleran Ice Sheet generally melted from offshore-to-mainland, and from mountaintops-to-valley bottoms (Clague and James, 2002). Glacial valleys and fjords like the Douglas Channel became ice-free after the majority of the coastal margin. During the LGM, Douglas

Channel was completely glaciated and the ice margin was over 100 km away offshore. Glacial ice on Haida Gwaii was connected to the mainland Cordilleran Ice Sheet by a major ice lobe that flowed through the Dixon Entrance, and several ice tongues crossed the continental shelf in Queen Charlotte Sound (Shaw et al., 2020: Fig. 12). There may have been ice-free refugia in the southern Hecate Strait and between the Queen Charlotte Sound ice tongues, but the mainland was likely completely frozen (Mathewes and Clague, 2017; Shaw et al., 2020). With the onset of deglaciation, the ice retreated inland, though submarine moraines identified in multibeam bathymetry outside the islands on the eastern edge of the Hecate Strait suggest a pause in ice retreat before it continued to the heads of the fjords, including Douglas Channel (Figs. 1 and 2; Shaw et al., 2020: Fig. 14). There are several submarine moraines at intervals up the Channel, which are likely associated with pauses in glacial retreat or re-advances (Fig. 1B) (Bornhold, 1983; Shaw et al., 2017, 2020). One of these moraines forms a sill across the Douglas Channel just south of the mouth of Kitkiata Inlet, in the center of our study area (Fig. 1B).

This sequence of northern Northwest Coast deglaciation lacks robust absolute dating; however a handful of dates from the broader region provide constraints for the inland glacial retreat (Fig. 2; Shaw et al., 2020). <sup>10</sup>Be dating of bedrock and glacial erratics indicates that ice retreated from the western islands of Alexander Archipelago, 300 km northwest of the study area 17,000 years ago (Lesnek et al., 2018, 2020) and from the southwest side of Calvert Island, 230 km south 18,000 years ago (Darvill et al., 2018), marking the end of the LGM on the north coast. Shaw et al. (2020) hypothesize that the ice margin west of the mainland islands indicated by submarine moraines might be associated with a pause in retreat identified around Calvert Island between 17,600 and 16,600 years ago (Darvill et al., 2018). After that, ice withdrew from the mainland coast east of Calvert Island around about 14,500 years ago (Darvill et al., 2018; McLaren et al., 2014), though there may have been a brief re-advance in the area some time between 14,200 and 13,800 years ago (Eamer et al., 2017). Ice had withdrawn from most of the rest of the Alexander Archipelago by 15,000 years ago (Lesnek et al., 2020) and from the Prince Rupert area by at least 15,000–14,500 years ago (Letham et al., 2016). Between Prince Rupert and Calvert Island, ice retreat from the mouth of Douglas Channel is not directly dated, though Bornhold (1983:107) suggests it would have been ice-free around the same time as Prince Rupert.

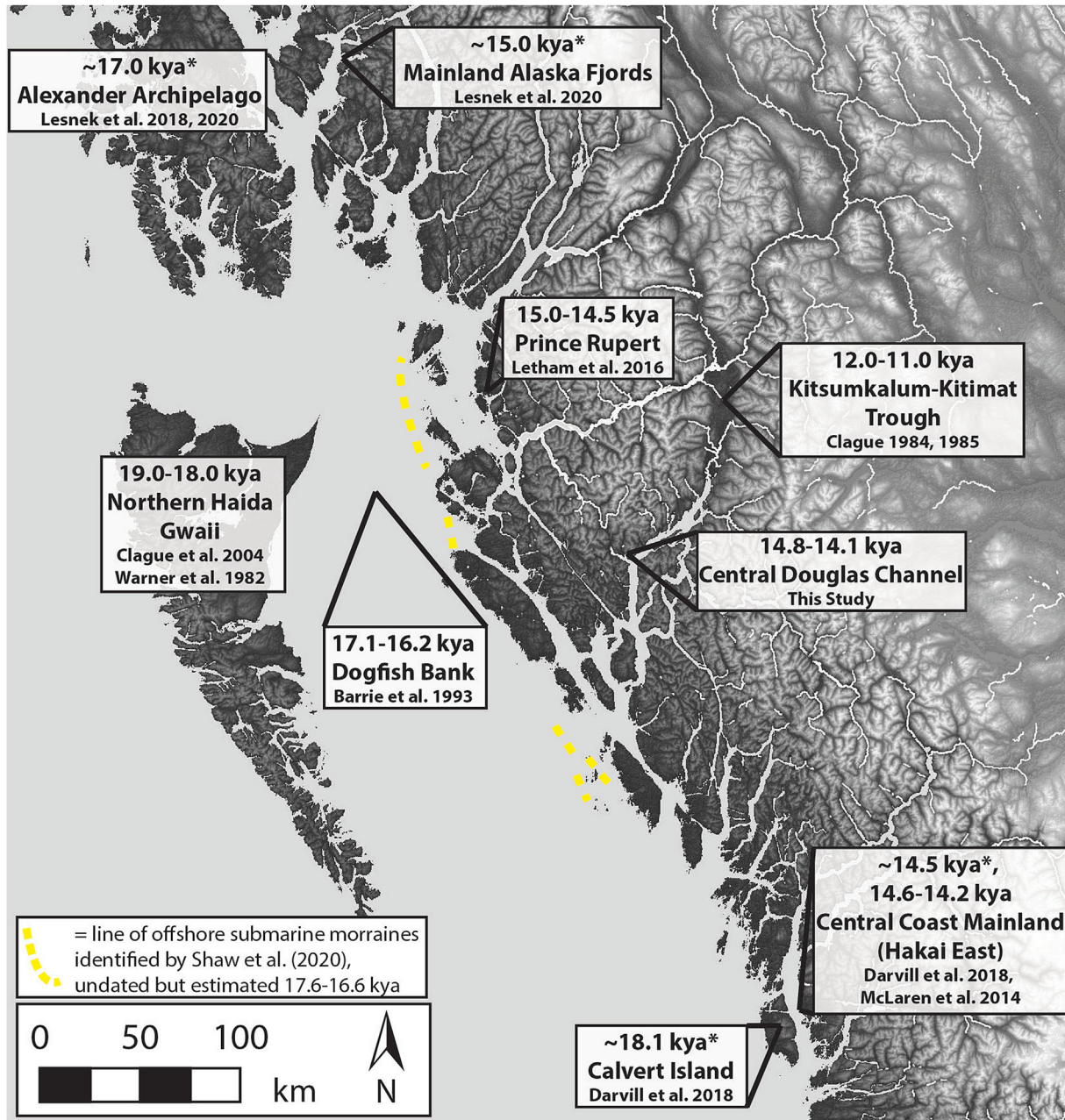


**Fig. 2.** Map of the northern Northwest Coast indicating select minimum ages for deglaciation following the Last Glacial Maximum. Ages indicated with an asterisk are approximate mean values from  $^{10}\text{Be}$  dating. Ages indicated with a range are rounded 2-sigma calibrated  $^{14}\text{C}$  ages. Data from Barrie et al., 1993; Clague, 1984, 1985; Clague et al., 2004; Darvill et al., 2018; Lesnek et al., 2018, 2020; Letham et al., 2016; McLaren et al., 2014; Shaw et al., 2020; Warner et al., 1982.

Radiocarbon dates on shells and wood from marine cores from the south end of Douglas Channel near Hawkesbury Island yielded calendar ages of 12,000 years (Conway and Barrie 2015, 2018), though new data from central Douglas Channel which we present below supports the inference of deglaciation of the mouth at or prior to 15,000 years ago. Clague (1984, 1985) proposes that an ice front indicated by a moraine at the city of Kitimat at the head of Douglas Channel indicates the fjord was fully ice-free by 12,500 years ago (reported as ~10.75 ka radiocarbon years BP by Clague), but that moraine is not directly dated. However, marine shells from Lakelse Lake, further north up the Kitsumkalum-Kitimat Trough

date to between 12,000 and 11,000 cal. BP, indicating that Douglas Channel was definitely ice-free by then (Fig. 2; Clague, 1984, 1985; Clague et al., 1982). The glacial stillstands or re-advances indicated by the submarine moraines in Douglas Channel would have occurred between ~15,000 BP and 12,000–11,000 BP, however they are currently undated. Bornhold (1983) and Shaw et al. (2017, 2020) propose that the Kitkiata sill is a moraine that was formed by a stabilized ice-front just south of Kitkiata Inlet around 13,800 years ago, however we demonstrate below that Kitkiata Inlet was already ice-free by this time and propose several alternative timings.

## 2. Data and methods

### 2.1. RSL limiting and index points

We collected various forms of data that either directly indicate (index points) or constrain (limiting points) the elevation of RSL position in the past (Table 2; [Hijma et al., 2015](#); [Shennan, 2015](#)). These include environmental transitions documented in sediment core samples from isolation basins, ancient remains of marine molluscs and coral *in situ* outside of their current normal tidal range, and archaeological sites indicating habitation on dry land at various elevations (Fig. 3). The reliability of these different forms of data varies depending on their susceptibility to post-depositional alteration, whereas the specificity of the inference about RSL position depends on the elevation range from which we might expect to find different proxies *in situ* (Table 2). Specificity is also impacted by our ability to measure accurate elevations and ages for each data point.

To develop an age-elevation curve of RSL through time we modified the measured elevations of samples according to their RSL indicative meanings (Table 2; [Hijma et al., 2015](#); [Shennan, 2015](#)). The indicative meaning describes where a RSL index or limiting point formed relative to tidal levels; indicative meanings are derived from the vertical distributions of modern RSL indicators (see [Shennan, 2015](#) for detailed explanation; also [van de Plassche, 1986](#)). For most limiting points, we follow [Engelhart et al. \(2015\)](#) and conservatively assume that freshwater or terrestrial (upper) limiting points originated above MTL and marine (lower) limiting points originated below MTL (see Table 2 for more specific indicative meanings that could be used to further refine indicative range). For some marine limiting points derived from remains of organisms with known maximum habitat tidal elevations we have adjusted the elevations of RSL indicated by each accordingly (see section 2.4 below and Table 2). For upper limiting points from archaeological occupation sites we assume an indicative meaning of above high tide levels. By plotting the elevations of seven index points and 61 limiting points against their measured radiocarbon ages, we are able to estimate a curve of sea level position through time for the last 14,500 years for the study area.

### 2.2. Measuring elevation and age

The “zero” datum for all elevations in this study is the Canadian Geodetic Vertical Datum of 1928 (CGVD28), a measure of geodetic mean sea level used by the Canadian Hydrographic Survey for tidal parameters. We report elevations relative to CGVD28 as “m asl” – meters above sea level. For RSL data that indicate certain tidal ranges, we used the tidal parameters for the nearest Canadian Hydrographic Survey Benchmark Station, Station #9130 at Hartley Bay, 25 km south of Kitkiata Inlet (Table 1, Fig. 1B). CGVD28 is 2.921 m above chart datum at Hartley Bay; Table 1 includes elevations of tidal parameters relative to geodetic mean sea level that are relevant to the indicative meanings of RSL data. The Hartley Bay tide station is the closest to our study area; we assume these tidal parameters are applicable up to central Douglas Channel and that they have been constant through time.

Elevations were measured in the field using a combination of methods, either against a local datum established with an Emlid Reach RS RTK GPS or relative to the barnacle line. For elevations derived from RTK measurements we logged >1 h of satellite data at a base station and used Natural Resources Canada's Precise Point Positioning tool (NRCCN PPP; <https://webapp.geod.nrcan.gc.ca/geod/tools-outils/ppp.php>) to post-process the observations. For measurements relative to the barnacle line we assume that barnacle line =  $1.65 \pm 0.30$  m asl, which was calculated through

repeated RTK measurements in the Prince Rupert area (K. Superant, personal communication 2015). Elevations were measured relative to these datum points using a laser range finder. In many instances, elevations were derived by overlaying hand-held Garmin GPS positions recorded in the field over a 1 m cell-size bare earth LiDAR digital terrain model (DTM) acquired by the University of Northern British Columbia and Hakai Institute. We took an average of pixel cell elevations within a 5 m buffer around each position to account for horizontal error in GPS measurements. Other elevation measurements were checked against the LiDAR for consistency. All elevations have been converted to CGVD28. Vertical measurement error ranges factoring in measurement uncertainties, tidal range, and instrument errors are applied to all data points in the final dataset and expressed as 95% confidence intervals (see [Hijma et al., 2015](#) for error types and equations).

The ages of all samples have been measured by AMS radiocarbon dating at the Keck Carbon Cycle AMS lab at the University of California Irvine. All results have been calibrated using OxCal 4.3 using the IntCal13 and Marine13 calibration curves ([Bronk Ramsey, 2009](#)), and are presented as 2-sigma calibrated probability ranges of years Before Present (BP = 1950). In cases where dateable material was scant or fragmented we dated bulk samples; these have an additional error range of  $\pm 100$  years applied before calibration ([Törnqvist et al., 2015](#)). For marine samples we accounted for the marine reservoir effect (MRE) by using a  $\Delta R$  of  $273 \pm 38$ , which has been calculated for the Prince Rupert Harbour area for use with the Marine13 calibration curve ([Edinborough et al., 2016](#)). MRE can vary with time and space ([Hutchinson et al., 2004b](#); [Martindale et al., 2018](#)), but no local assessments have been made for the Douglas Channel. The Prince Rupert  $\Delta R$  is the most robustly calculated value for the north coast region, and it accords well when applied to our data, so we chose it as a best estimate. In one instance, we dated megaspores from *Isoetes* sp. (likely quillwort), a genus made up of mostly aquatic plant species. Aquatic plants are susceptible to old carbon reservoir effects if the bedrock is rich in carbonates ([Marty and Myrbo, 2014](#)). In our study area most of the bedrock is plutonic igneous rock in which we expect very little carbonate material; we therefore assume that a freshwater reservoir effect is negligible for aquatic plant samples.

In cases where we have stratigraphically-sequenced dated samples with ages in close succession we use Sequence Modelling in OxCal 4.3 ([Bronk Ramsey, 2009](#)) to refine our calibrations and test for outliers. This modelling uses Bayesian statistics to narrow the calibrated age ranges of radiocarbon dates using information from dated samples above and below each date. In text and in figures we present modelled ages; both modelled and unmodelled ages are presented in the [Supplemental Table 1](#).

Several dates had to be rejected from our final dataset on the grounds that they were obvious outliers or were contradicted by multiple other lines of evidence. These are listed in [Supplemental Table 2](#) along with rationale for rejection. They are not referred to in the following analysis.

### 2.3. Isolation basin sediment cores

We collected core samples from isolation basins (water-filled topographical basins where sediment containing proxies for shifts in the elevation of sea level accumulate in vertical succession through time; [Kjemperud, 1981](#); [Long et al., 2011](#); [Shennan et al., 1994](#)) using a Livingstone piston corer ([Wright, 1967](#)). When submerged below relative sea level, isolation basins will accumulate marine sediment; if RSL falls below the elevation of the sill of the basin – thus isolating the basin from the ocean – sediment from brackish transitional conditions and then freshwater conditions will be deposited on top of the marine sediment (Fig. 3). Core

**Table 2**

RSL data point types used in the present study and descriptions of indicative meanings. See Table 1 for explanation of tidal parameters and their values for the study area. See Shennan (2015) and Hijma et al. (2015) for a detailed explanation of Indicative Range, Indicative Meaning, Reference Water Level, and how to apply these to the measured elevations of sea level indicators.

Indicator Sample Type	Indicative Meaning	Indicative Range	Reference Water Level	Explanation	Reliability and Specificity as RSL Indicator
<b>Index Points</b>					
Upper transitional (mixed fresh and brackish/marine diatom assemblage in isolation basin sediments)	Basin sill is either nearly below high tide influence (dropping RSL) or just being inundated by high tides (rising RSL)	HAT to MTL	(HAT + MTL)/2	Conservatively assumes that the dated sample represents the time at which the sill of the basin was between mean tide level and the highest astronomical tide level and was on the verge of being isolated/inundated (Engelhart et al., 2015; Hijma et al., 2015).	Moderately-to-highly reliable, highly specific
Low lagoon (basin with mixed fresh and brackish/marine assemblage but dominated by brackish diatoms)	Basin sill is below mean tide level but is occasionally isolated during low tides.	MTL to LAT (MTL + LAT)/2		Conservatively assumes that the dated sample represents deposition between the lowest astronomical tide level and mean high water level. Implemented in this study for a lagoon where we could compare ancient diatom assemblages with near-present assemblages.	Moderately-to-highly reliable, highly specific
Upper salt marsh sediment in isolation basin core or geological exposure indicated by halophilic diatoms in sandy peat	Sediment was deposited in salt marsh conditions at the upper extremes of the tidal range.	HAT to HWMT	(HAT + HWMT)/2	Conservatively assumes that the dated sample represents deposition between the highest astronomical tide level and mean high water level (Engelhart et al., 2015; Hijma et al., 2015).	Highly reliable, highly specific (if from an isolation basin)
Undifferentiated salt marsh sediment in isolation basin core or geological exposure indicated by mixed fresh-halophilic-brackish diatoms in sandy peat	Sediment was deposited in salt marsh conditions	HAT to MTL	(HAT + MTL)/2	Conservatively assumes that the dated sample represents deposition between the highest astronomical tide level and mean tide level, generally the elevation within which salt marshes form (Engelhart et al., 2015; Hijma et al., 2015).	Moderately-to-highly reliable, highly specific
<b>Limiting Points</b>					
<b>Indicative Meaning (Conservative Option used in present study following Engelhart 2015; Hijma et al. 2015:538)</b>					
Marine shells in sediment, not in growth position	Conservative: indicator formed below MTL. Specific: Sediment with shell is from within or below the tidal range.		<MTL		Highly reliable, not specific
Growth position <i>Saxidomus gigantea</i> (butter clam) shells	The <i>S. gigantea</i> specimen was at or below LLWMT +0.5 m when it was alive: <i>S. gigantea</i> prefers to live between LLWMT +0.5 m and LLWMT -1.0 m (Chew and Ma, 1987; Foster, 1991; i.e. -1.4 to -2.8 m asl in study area), but can live up to at least 10 m below LLWMT (Bourne and Quayle, 1972). See text for details.		<LLWMT +0.5 m		Moderately reliable, highly specific if a contextual argument can be made that the specimens were alive in their preferred tidal range.
Growth position <i>Nuculana pernula</i> shells	RSL was at least 20 m higher than the elevation of the <i>N. pernula</i> specimen when it was alive ( <i>N. pernula</i> typically lives in muddy environments at water depths greater than 20 m below sea level; Coan et al., 2000).		<MSL +20		Moderately reliable, low specificity
<i>Caryophyllia arnoldi</i> coral adhered to bedrock	RSL was 40–656 m higher than the elevation of the coral specimen when it was alive ( <i>C. arnoldi</i> lives between 40 and 656 m below sea level; Cairns, 1994).		<MSL +40		Highly reliable if adhered to bedrock, low specificity
Only brackish/marine diatoms in sediments	Conservative: indicator formed below MTL. Specific: Sediment was deposited in coastal/marine setting, or, in the case of isolation basin sediments, when the sill was below lowest tide level.		<MTL		Highly reliable (if from an isolation basin), low specificity
Only freshwater diatoms in sediments	Conservative: indicator formed below MTL. Specific: Sediment was deposited in fully freshwater setting, or, in the case of isolation basin sediments, when the sill was above highest tide level.		>MTL		Highly reliable (if from an isolation basin), low specificity. Not reliable if sediment has slumped.
Terrestrial sediment (e.g., peat/paleosol)	Conservative: indicator formed below MTL. Specific: Sediment was formed/deposited above high tide.		>MTL		Moderately-to-highly reliable, low specificity. Not reliable if sediment has slumped.
Archaeological site with remains of habitation (shell midden, charcoal concentrations, architectural features)	Indicator formed above HHWMT. Lowest instance of archaeological material was likely deposited above high tide.		>HHWMT		Moderately reliable (archaeological material can be moved into secondary contexts by cultural or natural agents), low specificity

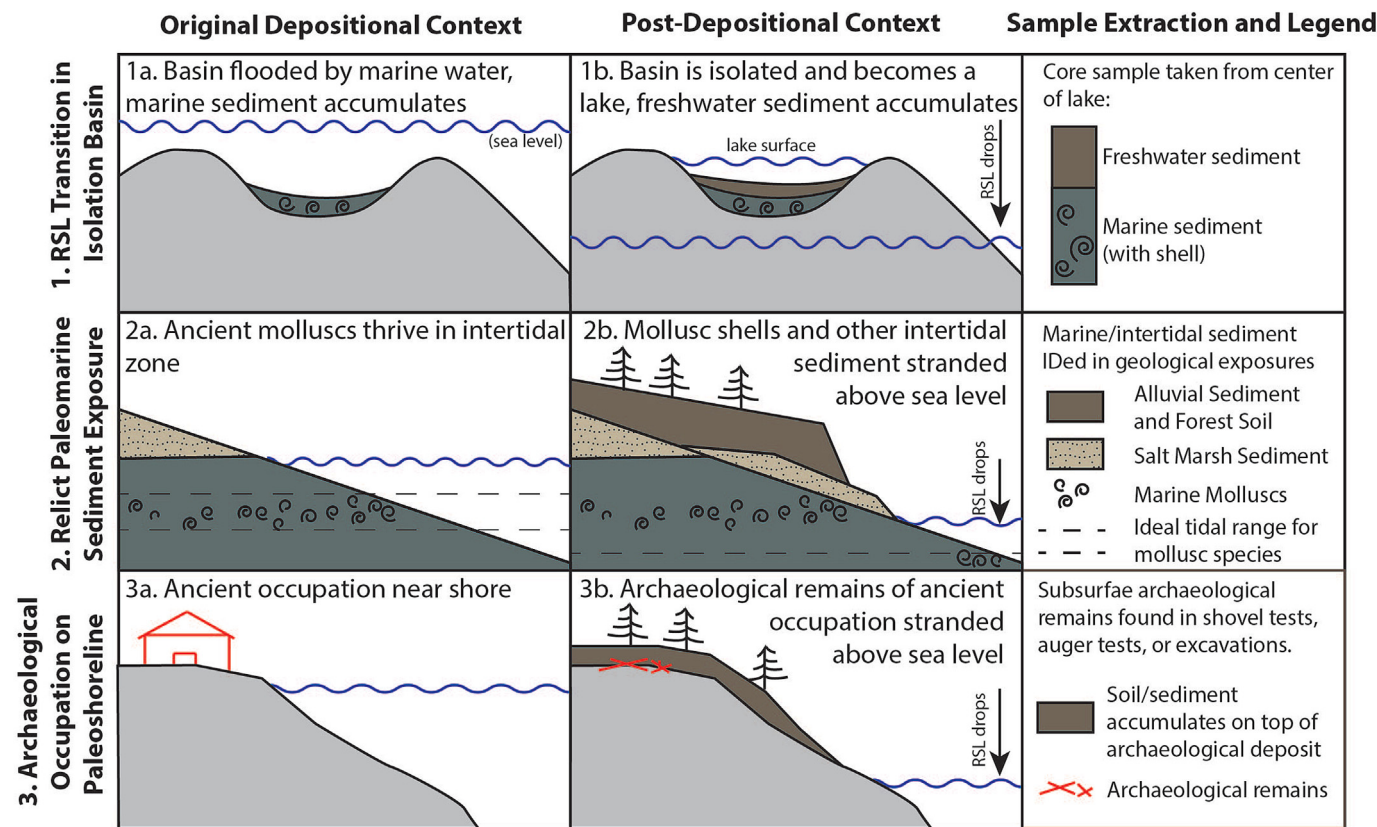


**Fig. 3.** Schematic of RSL-constraining data types used to create the Central Douglas Channel relative sea level curve.

samples from isolation basins contain this vertical stratigraphic sequence of environmental change. By identifying and radiocarbon dating transitions from marine conditions to freshwater conditions (or vice versa in the case of rising RSL) we can assess when the RSL passed over the elevation of the basin. Because isolation basin sills are fixed in space, RSL information from these cores can be both highly reliable and highly specific (Table 2).

To identify environmental transitions in the core samples, we logged sediment characteristics and analyzed the microfossil silica cell walls of diatoms preserved within the sediment. Different diatom species are sensitive salinity indicators; marine-brackish-fresh water transitions are usually readily identified based on changes in diatom assemblages (Battarbee, 1986; Zong and Sawai, 2015). We sampled sediment for diatom analysis at intervals across the core length but focused around changes in visible sediment characteristics (often indicative of changes in depositional environment). We narrowed down on transitions in the salinity iteratively through diatom identification, usually getting to a point of sampling every 2 cm around a transition. We prepared the samples using established methods (Letham et al., 2016) and performed identifications under 400x and 1000x magnification using various reference guides (Campeau et al., 1999; Fallu et al., 2000; Foged, 1981; Hein, 1990; Krammer and Lange-Bertalot, 1986a, b, c, d; Laws, 1988; Pienitz et al., 2003; Rao and Lewin, 1976; Tynni, 1986; Witkowski et al., 2000). We attempted to obtain a minimum of 300 identifications per sample, or at least 10 horizontal "passes" over a slide when diatoms were rare. We classified diatoms into a five-part salinity scheme based on the halobian system (Hustedt, 1953; Kolbe, 1927, 1932) outlined by Zong and Sawai (2015:234): 1 = halophobic (salt intolerant freshwater) species, 2 = oligohalobous indifferent (freshwater) species,

3 = oligohalobous halophilic (freshwater but tolerant of salinity levels up to 2‰) species, 4 = mesohalobous (brackish water with salinity levels ranging from 2‰ to 30‰) species, and 5 = polyhalobous (marine water with salinity > 30‰) species.

#### 2.4. Paleomarine exposures

We surveyed riverbanks for areas where the river has incised through alluvial sediment and exposed sections of marine sediment. Veneers of glacio-marine clay and terminal Pleistocene- and early Holocene-aged marine mud and sand are ubiquitous in the study area and are well preserved in the valley and fjord bottoms beneath later Holocene sediments, often at elevations well above current sea level. Many of the paleomarine deposits contain remains of marine shellfish. Dates from these shell beds provide marine limiting RSL information (Fig. 3). However, such deposits lack the same elevation constraints as isolation basins with fixed sills, and are thus less reliable and can be less specific RSL indicators (Table 2). Furthermore, post-depositional altering of the position of these shells or the entire deposits, such as bioturbation, erosion, uplift/subsidence, compaction, or slumping can reduce the reliability of these data for inferring RSL.

We identified many exposures of marine sediment with abundant marine bivalves preserved in growth position above their tidal range relative to today's tides in the Quaal River Valley and the upper intertidal zone of Kitkiata Inlet. We use the preferred habitat elevation ranges for certain species to narrow down the RSL indicative range of these specimens. For example, *Nuculana pernula* live below ~20 m asl (Coan et al., 2000); we therefore add 20 m to the measured elevation of growth position specimens to derive its indicative meaning (see Table 2). Butter clams (*Saxidomus gigantea*)

live deeper than LLWMT +0.5 m (i.e. below  $-1.4$  m asl in our study area; Chew and Ma, 1987; Foster, 1991). To calculate the RSL marine limiting indicative meaning of *S. gigantea* shells found in growth position we add 1.4 m to their measured elevations (Table 2). This is a more conservative approach than others who have used growth position *S. gigantea* shells as index points (e.g. Carlson and Baichtal, 2015; Letham et al., 2016), because our samples are gathered from a geomorphologically active area with a potential for post-depositional downward movement of soft sediment RSL indicators (see Discussion).

Furthermore, the potential slumping of exposures in the Quaal River Valley means that freshwater- or terrestrially-deposited indicators overlying raised marine sediments cannot be used reliably as upper RSL limiting information. Dates on samples overlying marine deposits in exposures are used to make paleoenvironmental inferences, but they are not included in the final RSL reconstruction.

### 2.5. Basal dates from archaeological sites

We use radiocarbon dates from the basal layers of archaeological habitation sites as upper limiting RSL data (Fig. 3). We assume that human occupation took place above or near higher high water mean tide for the time (HHWMT = 2.2 m asl; Table 1). If this archaeological material has not been disturbed, these data can be reliable RSL indicators. However, because people could theoretically live anywhere above high tide, they are not specific indicators (Table 2). Several of the archaeological sites in this study were identified on landforms associated with raised paleoshorelines identified using LiDAR-derived DTMs (see Letham et al., 2018 for methods). These are the first-published radiocarbon dates for archaeological sites anywhere in the Douglas Channel region.

## 3. Results

Sixty-eight index and limiting points from 31 different locations constrain our RSL curve for the Central Douglas Channel region (Fig. 4, Table 3). In addition to presenting these data here, we also contribute a version formatted to be consistent with the HOLSEA Working Group's Global Sea Level Atlas (Khan et al., 2019) in Supplemental Table 3. Most of the data come from the Quaal/Kitkiata watershed. However, because of the paucity of ideal sample locations (particularly for isolation basin cores) in the steep sided valleys, we also collected data from Kishkosh Inlet (~10 km south) and Hartley Bay area (~25 km south) to fill in sampling elevation gaps (see Fig. 4). This broad sampling strategy has the potential to introduce spatial variation into our dataset, which we address in the Discussion.

### 3.1. Isolation basin sediment cores

We collected core samples from seven basins ranging from +90 to  $-1.35$  m asl (Table 4). The higher elevation cores indicate higher RSL immediately after deglaciation and constrain RSL regression towards modern elevations. Results of diatom analyses on these cores are presented in the core diagrams (Figs. 5–11) and Supplemental Table 4.

#### 3.1.1. White River Lake cores (WRL#1 and WRL#2; Quaal/Kitkiata watershed)

White River Lake (informal name), nestled in the ridge dividing the Quaal River Valley from the Kitkiata River Valley, flows out over a  $90 \pm 0.23$  m asl sill. At the bottom of cores from this lake we encountered impenetrable rock that we interpret as either till or bedrock. The rock is overlain by glaciomarine sediment with flecks

of marine shell, a brief transition zone with brackish diatoms, and then freshwater gyttja (Fig. 5, Table 4). A marine shell from just below the transition dates to 14,512–14,028 cal. BP (UCIAMS-216113, marine limiting), and deciduous tree leaf parts preserved just above this transition date to 14,115–13,484 cal. BP (UCIAMS-216105, freshwater limiting). The older age indicates that the study area was deglaciated by at least 14,500–14,000 years ago and that RSL was above 90 m asl at this time, and the leaf date indicates that RSL had dropped below 90 m asl by between 14,100–13,500 years ago. Furthermore, given that this is the highest elevation sample in our dataset, it helps constrain and interpret other early lower elevation limiting data (see below).

#### 3.1.2. Xaa Usta'a Pond core (XUP#4; Quaal/Kitkiata watershed)

Xaa Usta'a Pond (local Gitga'at name) is in an open area of bogland with several ponds nestled in an isolation basin with a  $67 \pm 0.61$  m asl bedrock sill. Core XUP#4 contains mottled blue-gray silty clay overlain by brown organic-rich silt, then sandy-silty peat to the top (Fig. 6, Table 4). The entire core contained abundant and diverse freshwater diatoms with no indication of marine influence.

The only readily collected plant macrofossils at the base of the core were tiny rootlets and spherical *Isoetes* sp. megaspores. A bulk sample of multiple megaspores returned freshwater limiting age of 13,306–12,771 cal. BP (UCIAMS-210408). The freshwater diatoms indicate that RSL had dropped below 67 m asl before 13,000 BP. The marine sediment at 90 m asl in White River Lake indicates that Xaa Usta'a pond was once inundated by the ocean, but sediment from that time was not captured in our core.

#### 3.1.3. Kishkosh Bog-Pond core (KBP#3; Kishkosh Inlet)

Kishkosh Bog-Pond (informal name) is a small pond that flows out over a poorly defined  $21.9 \pm 0.57$  m asl sill. The base of core KBP#3 contains gray sand, silt, and clay layers with no diatoms at the base, increasing upwards to rarely occurring *Diploneis interrupta* specimens (a mesohalobous diatom species often found in salt marshes or sandy intertidal flats; Fig. 7, Supplemental Table 4). This minerogenic sediment is capped by a sharp transition to sandy peat with a mixture of salt-tolerant oligohalobous and mesohalobous species, indicative of a coastal salt marsh environment, overlain by peat with freshwater diatoms (Fig. 7, Table 4, Supplemental Table 4). The diatom transition indicates falling RSL and a transformation from an intertidal salt marsh to a freshwater pond. A twig from the upper side of the transition from peat to sandy peat and the uppermost instance of salt-tolerant diatoms dates to 10,152–9743 cal. BP (UCIAMS-201808, index point: high salt marsh). This date indicates high salt marsh conditions or nearshore conditions a little ways above high tide around 10,000 years ago.

#### 3.1.4. Kitkiata Lake cores (KITL#2 and KITL#3; Quaal/Kitkiata watershed)

Kitkiata Lake flows over a  $21.5 \pm 0.23$  m asl sill into the Kitkiata River, which drains into Kitkiata Inlet. The sill elevation is a minimum, as the south end of the lake abuts a ridge perpendicular to the river valley that may be a moraine through which the Kitkiata River has incised through time. Cores KITL#2 and KITL#3 have marine sediments with shell and marine diatoms at the base dating 11,811–11,376 cal. BP (UCIAMS-226971, marine limiting) and 11,703–11,298 cal. BP (UCIAMS-226958, marine limiting) (Fig. 8, Table 4). A transition to brackish conditions is characterized by laminated clay overlain by organic rich silt with predominantly brackish diatoms. A conifer needle from the brackish silt yielded an age of 11,591–11,245 cal. BP (UCIAMS-226960, index point: isolation basin upper transitional) indicating that RSL was higher than

**Table 3**

Radiocarbon dated RSL Data Points used for reconstructing the central Douglas Channel RSL curve. Calibrated ages indicated with asterisks have been modified with an additional  $\pm 100$  years for bulk samples (following Törnqvist et al., 2015).

Map ID (see Fig. 4)	UCIAMS Lab Number	Site Context	Dated Material	14C Age BP	+/-	Calendar Range BP (older, 2 sigma)	Calendar Range BP (recent, 2 sigma)	Cal. BP Median	Proxy Indicator	Data Point Type	Sample Elevation/Sill Elevation (m asl, CGVD28)	Sample RSL Indicative Range (Index Points) or Indicative Meaning (limiting points)	Total Elevation Error (+/- m)	
<b>Isolation Basin Sediment Cores</b>														
WRL#2	230961	White River Lake	Livingstone Core WRL#1, 429 cm	bark/wood	10620	35	12695	12545	12611	freshwater diatoms	upper limiting	90	89.7 m (>MTL)	0.23
WRL#2	216105	White River Lake	Livingstone Core WRL#2, 456 cm	leaf fragments	11895	35	14115*	13484*	13803	freshwater diatoms	upper limiting	90	89.7 m (>MTL)	0.23
WRL#2	216113	White River Lake	Livingstone Core WRL#2, 460 cm	clam shell	12980	25	14512	14028	14234	marine shell in sandy silt	lower limiting	90	89.7 m (<MTL)	0.23
XUP#4	213801	Xaa Usta'a Pond	Livingstone Core XUP#4, 6 cm	conifer needles	1060	20	1049	928	963	freshwater diatoms	upper limiting	67	66.7 m (>MTL)	0.61
XUP#4	201809	Xaa Usta'a Pond	Livingstone Core XUP#4, 81 cm	conifer needle	8150	30	9243	9009	9076	freshwater diatoms	upper limiting	67	66.7 m (>MTL)	0.61
XUP#4	210408	X'a a Usta'a Pond	Livingstone Core XUP#4, 100–104 cm	Isoetes sp. megaspores	11205	30	13306*	12771*	13054	freshwater diatoms	upper limiting	67	66.7 m (<MTL)	0.61
KBP#3	201808	Kishkosh Bog/Pond	Livingstone Core KBP#3, 15 cm	Twig	8840	30	10152	9743	9923	halophilic diatoms	index (upper salt marsh)	21.9	20.6–17.9 m asl (IR=HAT to HWMT)	0.57
KITL#3	226959	Kitkiata Lake	Livingstone Core KITL#3, 228 cm	conifer needle	5770	15	6635	6504	6575	freshwater diatoms	upper limiting	21.5	21.2 m (>MTL)	0.23
KITL#3	226957	Kitkiata Lake	Livingstone Core KITL#3, 433 cm	wood fragment	9470	25	11062	10603	10745	freshwater diatoms	upper limiting	21.5	21.2 m (>MTL)	0.23
KITL#3	226960	Kitkiata Lake	Livingstone Core KITL#3, 451 cm	conifer needle	10080	80	11591	11245	11407	brackish diatoms	index (isolation basin transition)	21.5	21.5–17.9 m asl (IR=HAT to MTL)	0.23
KITL#3	226958	Kitkiata Lake	Livingstone Core KITL#3, 461 cm	mixed plant matter	9925	30	11703	11298	11498	marine shell flecks, marine diatoms	lower limiting	21.5	21.2 m (<MTL)	0.23
KITL#3	226971	Kitkiata Lake	Livingstone Core KITL#3, 466.5 cm	barnacle shell	10700	20	11811	11376	11603	marine shell in sand	lower limiting	21.5	21.2 m (<MTL)	0.23
LGL#2	213798	Lower Gabion Lake	Livingstone Core LGL#2, 253 cm	conifer needle	8440	120	9691	9141	9448	freshwater diatoms	upper limiting	13.8	13.5 m (>MTL)	0.35
LGL#2	213799	Lower Gabion Lake	Livingstone Core LGL#2, 289 cm	twig/wood	8710	90	9942	9531	9725	brackish diatoms	index (isolation basin transition)	13.8	13.8–10.2 m asl (IR = HAT to MTL)	0.35
K	163682	Lower Gabion Lake	Grab sample from lake bed	marine shell	9490	20	10162	9859	10007	marine shell	lower limiting	13.8	13.5 m (<MTL)	0.61
DGBT#1	213795	D'boigyet Lake	Livingstone Core DBGT#1, 215 cm	conifer needle	2855	20	3054	2882	2963	freshwater diatoms	upper limiting	7.9	7.6 m (>MTL)	0.27
DGBT#1	213796	D'boigyet Lake	Livingstone Core DBGT#1, 220 cm	conifer needle fragments (multiple)	2850	20	3230*	2892*	3043	brackish diatoms	index (isolation basin transition)	7.9	7.9–4.2 m asl (IR = HAT to MTL)	0.27
DGBT#1	213797	D'boigyet Lake	Livingstone Core DBGT#1, 415 cm	Twig	4165	20	4827	4619	4715	marine shell and brackish-marine diatoms	lower limiting	7.9	7.6 m (<MTL)	0.27
DGBT#1	206795	D'boigyet Lake	Livingstone Core DBGT#1, 978 cm	clam shell	8090	25	8372	8176	8279	marine shell in sand, lower limiting	7.9	7.6 m (<MTL)	0.27	
DGBT#1	206790	D'boigyet Lake	Livingstone Core DBGT#1, 978 cm	Twig	7495	20	8380	8213	8329	marine shell in sand, lower limiting	7.9	7.6 m (<MTL)	0.27	
KL#2	230960	Kishkosh Lagoon	Livingstone Core KL#2, 70 cm	wood	1605	20	1550	1415	1480	brackish and marine diatoms, similar to lagoon current condition assemblage	index (lower lagoon)	-1.35	1.5 to -1.35 m asl (IR = MTL to LAT)	0.6
KL#2	210398	Kishkosh Lagoon	Livingstone Core KL#2, 84 cm	Wood	1795	15	1813	1631	1725	brackish and marine diatoms, similar to lagoon	index (lower lagoon)	-1.35	1.5 to -1.35 m asl (IR = MTL to LAT)	0.6

(continued on next page)

Table 3 (continued)

Map ID (see Fig. 4)	UCIAMS Lab Number	Site Number	Sample or Test Type, Number, and Context	Dated Material	14C Age BP	+/- Calendar Range BP (older, 2 sigma)	Calendar Range BP (recent, 2 sigma)	Cal. BP Median	Proxy Indicator	Data Point Type	Sample Elevation/Sill Elevation (m asl, CGVD28)	Sample RSL Indicative Range (Index Points) Indicative Meaning (limiting points)	Total Elevation Error (+/- m)		
current condition assemblage															
KL#2	213789	Kishkosh Lagoon	Livingstone Core KL#2, 87 cm	mussel shell	11955	30	13307	13054	13175	marine shell in blue gray clay	lower limiting	-1.35	-1.62 m (<MTL)	0.6	
KL#2	213790	Kishkosh Lagoon	Livingstone Core KL#2, 115 cm	clam shell	8660	25	9091	8797	8967	marine shell in sand and clay	lower limiting	-1.35	-1.62 m (<MTL)	0.6	
KL#2	210399	Kishkosh Lagoon	Livingstone Core KL#2, 119 cm	small conifer cone	8170	20	9245	9023	9101	marine shell in sand	lower limiting	-1.35	-1.62 m (<MTL)	0.6	
KL#2	213802	Kishkosh Lagoon	Livingstone Core KL#2, 123 cm	wood (cone fragment)	8500	25	9535	9477	9507	marine diatoms	lower limiting	-1.35	-1.62 m (<MTL)	0.6	
KL#2	201810	Kishkosh Lagoon	Livingstone Core KL#2, 138 cm	Wood	10005	30	11695	11306	11475	unclear (no diatoms)	unclear (not used in RSL curve)	-1.35	No clear RSL relationship	0.6	
<b>Paleoceanic Exposures</b>															
H	195676	Ts'm Ga Lo'op, Kitkiata River	controlled sample from bedrock exposure	<i>Caryophyllia arnoldii</i> coral	13060	25	14750	14145	14439	coral	lower limiting	5.2	45.2 m asl ( <i>C. arnoldii</i> lives >40 m below RSL)	1.2	
I	225534	Upper Kitkiata Paleoceanic Exposure	controlled sample from exposure, uppermost observed shell	marine shell	11710	30	13051	12745	12894	marine shell and foraminifera	lower limiting	28	27.7 m (<MTL)	1.5	
J	195677	Quaal River Shell Exposure 2017-003	controlled sample from riverbank exposure	<i>Nuculana pernula</i> shell	11065	25	12481	12048	12267	marine shell in blue gray silt	lower limiting	2.3	22.3 m asl ( <i>N. pernula</i> lives >20 m below RSL)	1.1	
10	A	180101	Quaal River Shell Exposure 2016-004	controlled sample from top of shell bed in riverbank exposure	growth position <i>Saxidomus gigantea</i> shell	9490	20	10166	9882	10025	marine shell in blue gray silt	lower limiting	3.3	4.7 m asl ( <i>S. gigantea</i> live >1.4 m below RSL)	0.9
	B	180102	Quaal River Shell Exposure 2016-003	controlled sample from top of shell bed in riverbank exposure	growth position <i>Saxidomus gigantea</i> shell	9740	20	10455	10201	10315	marine shell in blue gray silt	lower limiting	2.6	4.0 m asl ( <i>S. gigantea</i> live >1.4 m below RSL)	0.8
	B	180105	Quaal River Shell Exposure 2016-003	controlled sample from top of shell bed in riverbank exposure	growth position <i>Saxidomus gigantea</i> shell	9805	20	10514	10245	10386	marine shell in blue gray silt	lower limiting	2.6	4.0 m asl ( <i>S. gigantea</i> live >1.4 m below RSL)	0.8
	C	201813	Quaal River Shell Exposure 2016-002	controlled sample from ~0.6 m above top of shell bed in riverbank exposure	conifer needle	3220	25	3544	3380	3429	freshwater diatoms	unreliable (not used in RSL reconstruction)	4	possible slumping, unreliable as upper limiting point	0.5
	C	180104	Quaal River Shell Exposure 2016-002	controlled sample from top of shell bed in riverbank exposure	growth position <i>Saxidomus gigantea</i> shell	10510	25	11347	11118	11228	marine shell in blue gray silt	lower limiting	3.4	4.8 m asl ( <i>S. gigantea</i> live >1.4 m below RSL)	0.5
D	180103	Quaal River Shell Exposure 2016-005	controlled sample from top of shell bed in riverbank exposure	growth position <i>Saxidomus gigantea</i> shell	9190	20	9686	9475	9573	marine shell in blue gray silt	lower limiting	1.7	3.1 m asl ( <i>S. gigantea</i> live >1.4 m below RSL)	0.75	

E	163681	Quaal River Shell Exposure 2015-001	controlled sample from middle of shell bed in riverbank exposure	barnacle shell	8960	15	9440	9238	9332	marine shell in blue gray silt	lower limiting	2.5	2.2 m (<MTL)	0.5
F	195668	Quaal River Shell Exposure 2017-001	in basal soil above alluvial sediment	Charcoal	1705	15	1692	1558	1608	charcoal in forest soil	upper limiting	7.8	7.5 m (>MTL)	0.4
F	213804	Quaal River Shell Exposure 2017-001	controlled sample from 1.1 ± 0.25 m above top of shell bed in riverbank exposure	twig with bark	8250	25	9285	9130	9204	unclear, possibly estuarine sediment	unreliable (not used in RSL reconstruction)	3.5	possible slumping, unreliable as RSL index point	0.5
F	201812	Quaal River Shell Exposure 2017-001	controlled sample from 0.35 ± 0.25 m above top of shell bed in riverbank exposure	conifer needle	8235	30	9312	9148	9247	mixed marine, brackish, and freshwater diatom assemblage	unreliable (not used in RSL reconstruction)	2.8	possible slumping, unreliable as RSL index point	0.5
G	210405	Xaa Usta'a Shell Exposure	controlled sample from bottom of Layer B, 100–105 cm DBS in riverbank exposure	conifer needle	695	20	674	567	647	salt marsh	index (undifferentiated salt marsh)	0.7	-1.1 m asl (IR = HAT to 0.2 MTL)	
G	210406	Xaa Usta'a Shell Exposure	controlled sample from Layer C, 105–120 cm DBS, cobble layer exposed in riverbank exposure	Wood	700	15	680	652	666	river cobbles	unreliable (not used in RSL reconstruction)	0.5	possible slumping, unreliable as RSL index point	0.2
G	210418	Xaa Usta'a Shell Exposure	controlled sample from Layer F, 149–162 cm DBS, well sorted gray silt with growth position clams in riverbank exposure	growth position <i>Saxidomus gigantea</i> shell	8700	20	9195	8925	9040	marine shell in blue gray silt	lower limiting	0.1	1.5 m asl ( <i>S. gigantea</i> live >1.4 m below RSL)	0.2
11	210407	Xaa Usta'a Shell Exposure	controlled sample from surface of Layer G, 162 cm DBS, flat laying wood on surface of shell death assemblage exposed in riverbank exposure	Wood	8365	15	9429	9299	9341	marine shells in sand, flat-lying wood and shells with barnacles attached	lower limiting	0.1	-0.2 m (<MTL)	0.2
G	210419	Xaa Usta'a Shell Exposure	controlled sample from Layer G, 162–183 cm DBS, shell death assemblage in riverbank exposure	growth position <i>Saxidomus gigantea</i> shell	8910	20	9445	9320	9376	marine shell in blue gray silt	lower limiting	0	1.4 m asl ( <i>S. gigantea</i> live >1.4 m below RSL)	0.2
G	210420	Xaa Usta'a Shell Exposure	controlled sample from Layer I, 235–250 cm DBS, gray silty clay with shells exposed in riverbank exposure	growth position <i>Saxidomus gigantea</i> shell	10155	25	11028	10705	10860	marine shell in blue gray silt	lower limiting	-0.7	0.7 m asl ( <i>S. gigantea</i> live >1.4 m below RSL)	0.2
IST-1	210417	Kitkiata Inlet Intertidal	intertidal shovel test (IST P004), 10 cm DBS	growth position <i>Saxidomus gigantea</i> shell	8505	20	8930	8600	8752	marine shell in sand	lower limiting	-0.3	1.1 ( <i>S. gigantea</i> live >1.4 m below RSL)	0.2
IST-2	201803	Kitkiata Inlet Intertidal	intertidal shovel test (IST, 2016–01), 5–10 cm DBS	growth position <i>Saxidomus gigantea</i> shell	9110	30	9592	9402	9492	marine shell in sand	lower limiting	-0.1	1.3 ( <i>S. gigantea</i> live >1.4 m below RSL)	0.2
IST-2	201804	Kitkiata Inlet Intertidal	intertidal shovel test (IST, 2016–01), 55 cm DBS	barnacle shell adhered to a whelk shell	9350	30	10003	9589	9789	marine shell in sand	lower limiting	-0.6	-0.9 m (<MTL)	0.2
IST-3	213791	Kitkiata Inlet Intertidal	intertidal shovel test (IST, 2018–08), 50 cm DBS	growth position <i>Saxidomus</i>	9105	25	9572	9403	9488	marine shell in sand	lower limiting	-1.3	0.2 ( <i>S. gigantea</i> live >1.4 m below RSL)	0.2

(continued on next page)

**Table 3** (continued)

Map ID (see Fig. 4)	UCIAMS Lab Number	Site Lab Number	Sample or Test Type, Number, and Context	Dated Material	14C Age BP	+/- Calendar Range BP (older, 2 sigma)	Calendar Range BP (recent, 2 sigma)	Cal. BP Median	Proxy Indicator	Data Point Type	Sample Elevation/Sill Elevation (m asl, CGVD28)	Sample RSL Indicative Range (Index Points) or Indicative Meaning (limiting points)	Total Elevation (+/- m)		
L	213786	Malsy Creek Paleoshell Exp. 2018-2	controlled sample from riverbank exposure, 5–6 m above barnacle line	<i>gigantea</i> shell clam shell	7255	20	7561	7411	7482	marine shell in sand	lower limiting	7.2	6.9 m (<MTL)	0.8	
<b>Archaeological Dates</b>															
3	180090	FjTh-21	shovel test, ST 2016–002, 37 cm DBS	charcoal	1160	15	1175	1000	1083	archaeological site	upper limiting	3.8	1.6 m asl (occupation above HHWMT)	0.3	
3	180091	FjTh-21	shovel test, ST 2016–023, 46–53 cm DBS	charcoal	1695	15	1688	1555	1595	archaeological site	upper limiting	4.6	2.4 m asl (occupation above HHWMT)	0.4	
8	180088	FjTh-22	shovel test, ST 2016–027, 130 cm DBS	charcoal	1750	15	1709	1614	1659	archaeological site	upper limiting	3.4	1.2 m asl (occupation above HHWMT)	0.6	
6	206786	FjTh-24	shovel test, ST 2018–011, 50 cm DBS	charcoal	4175	20	4829	4627	4724	archaeological site	upper limiting	10.0	7.8 m asl (occupation above HHWMT)	0.5	
6	206784	FjTh-24	shovel test, ST 2018–010, 48 cm DBS	charcoal	6655	20	7576	7495	7536	archaeological site	upper limiting	13.1	10.9 m asl (occupation above HHWMT)	0.3	
6	206785	FjTh-24	shovel test, ST 2018–010, 65–70 cm DBS	charcoal	7245	20	8158	8002	8067	archaeological site	upper limiting	12.9	10.7 m asl (occupation above HHWMT)	0.3	
2	206788	FjTh-25	shovel test, ST 2018–007, Layer C	charcoal	3840	20	4401	4152	4243	archaeological site	upper limiting	12.9	10.7 m asl (occupation above HHWMT)	0.5	
2	206789	FjTh-25	shovel test, ST 2018–007, 89 cm DBS	charcoal	4000	20	4521	4421	4474	archaeological site	upper limiting	12.7	10.5 m asl (occupation above HHWMT)	0.5	
2	206787	FjTh-25	shovel test, ST 2018–008, 58 cm DBS	charcoal	4755	20	5585	5336	5519	archaeological site	upper limiting	12.5	10.3 m asl (occupation above HHWMT)	0.5	
12	5	210400	FjTh-23	shovel test, ST 2018–012, 62 cm DBS	charcoal	965	20	930	797	855	archaeological site	upper limiting	3.2	1.0 m asl (occupation above HHWMT)	0.3
7	195664	FjTh-3	auger test, AT 2017–008, 80 cm DBS	charcoal	665	20	670	562	619	archaeological site	upper limiting	4.0	1.8 m asl (occupation above HHWMT)	0.5	
7	195661	FjTh-3	column sample from test pit, TP 2017 –004, 85–105 cm DBS	charcoal	990	15	952	803	913	archaeological site	upper limiting	4.2	2.0 m asl (occupation above HHWMT)	0.5	
7	180086	FjTh-3	shovel test, ST 2016–022, 120 cm DBS	charcoal	1295	15	1283	1183	1236	archaeological site	upper limiting	3.6	1.4 m asl (occupation above HHWMT)	0.6	
7	180087	FjTh-3	shovel test, ST 2016–020, 68 cm DBS	charcoal	1825	15	1816	1716	1765	archaeological site	upper limiting	6.9	4.7 m asl (occupation above HHWMT)	0.4	
7	225105	FjTh-3	shovel test, ST 2019–017, 60–75 cm DBS	charcoal	2735	20	2867	2778	2821	archaeological site	upper limiting	11.3	9.1 m asl (occupation above HHWMT)	0.4	
7	210403	FjTh-3	shovel test, ST 2018–016, 48 cm DBS	charcoal	2775	15	2927	2797	2868	archaeological site	upper limiting	10.3	8.1 m asl (occupation above HHWMT)	0.6	
7	210402	FjTh-3	shovel test, ST 2018–016, 28–35 cm DBS	charcoal	3325	15	3609	3482	3564	archaeological site	upper limiting	10.4	8.2 m asl (occupation above HHWMT)	0.6	
7	206782	FjTh-3	shovel test, ST 2018–014, Layer C	charcoal	5655	20	6486	6402	6436	archaeological site	upper limiting	15.6	13.4 m asl (occupation above HHWMT)	0.3	
7	206783	FjTh-3	shovel test, ST 2018–014, 70 cm DBS	charcoal	7715	20	8545	8430	8492	archaeological site	upper limiting	15.3	13.1 m asl (occupation above HHWMT)	0.3	
4	210401	FjTh-33	shovel test, ST 2018–018, 40–45 cm DBS	charcoal	3150	20	3445	3275	3376	archaeological site	upper limiting	7.2	5.0 m asl (occupation above HHWMT)	0.4	
1	201811	FjTh-9	excavation unit, House 2, 98 cm DBD	charcoal	420	25	520	335	494	archaeological site	upper limiting	2.4	0.2 m asl (occupation above HHWMT)	0.4	
1	206779	FjTh-9	excavation unit, House 9, 95 cm DBS	charcoal	1130	20	1072	969	1025	archaeological site	upper limiting	2.7	0.5 m asl (occupation above HHWMT)	0.6	

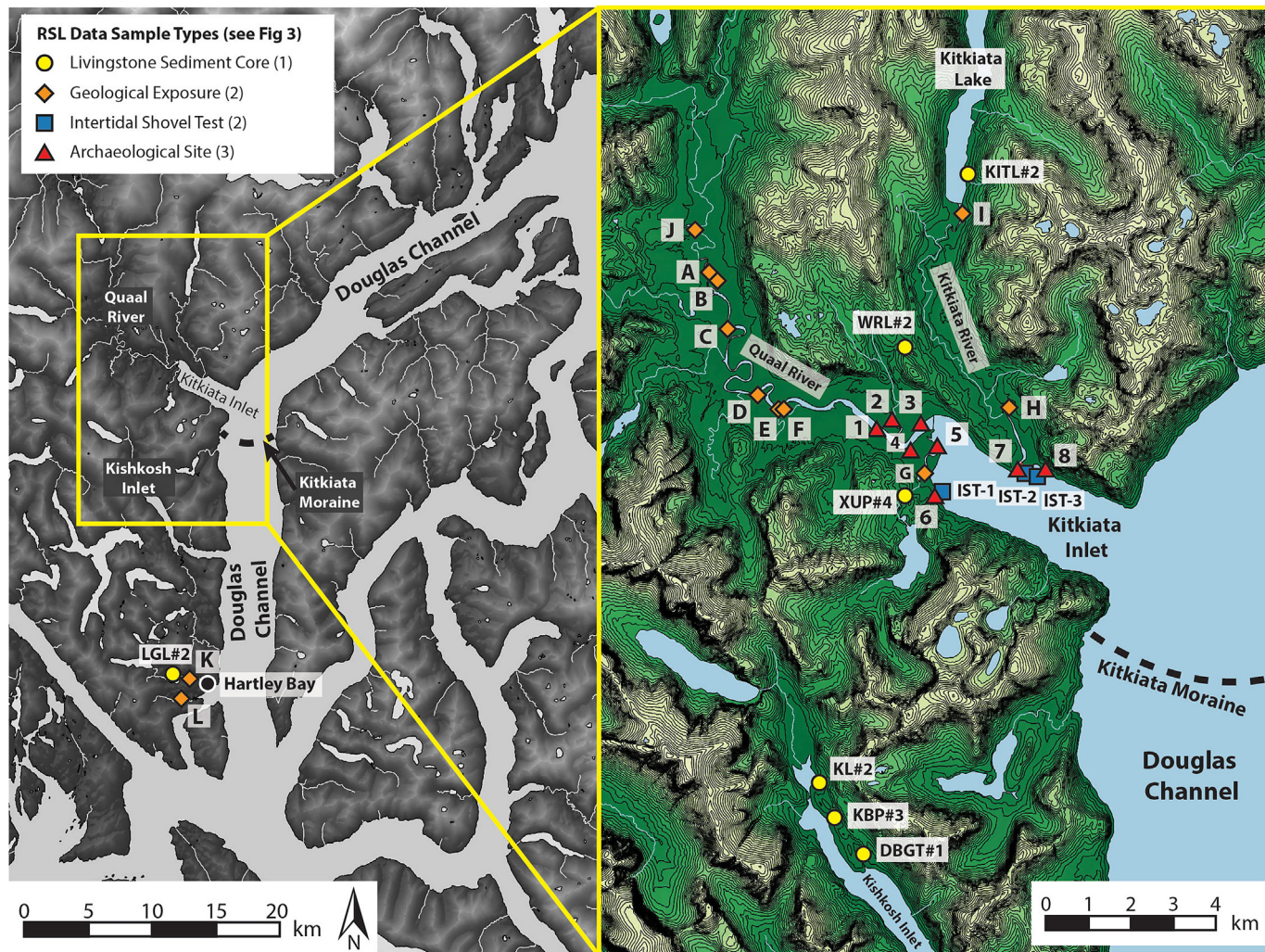


**Fig. 4.** Locations of data used to construct the Central Douglas Channel relative sea level curve. Data point type numbers in parentheses on the legend correspond with data point types in Fig. 3. Data point numbers and letters on the map correspond with radiocarbon dates in Table 3.

21.5 m until this time. This brackish silt is overlain by freshwater gyttja. Wood from the base of the gyttja dated 11,062–10,603 cal. BP (UCIAMS-226957, freshwater limiting), indicating that the lake had been fully isolated from marine influence by that time.

### 3.1.5. Lower Gabion Lake core (LGL#2; Hartley Bay)

Lower Gabion Lake outflows over a  $13.8 \pm 0.35$  m asl sill into a creek flowing to the ocean at Hartley Bay. *Saxidomus gigantea* shells in gray sand are exposed in patches beneath a thin veneer of freshwater gyttja in shallows at the east end of the lake. The *S. gigantea* shells indicate an extensive raised relict intertidal or high subtidal zone. One of these shells dated 10,164–9858 cal. BP (UCIAMS-163682, marine limiting). Core LGL#2 is from deeper water in the west end of the lake and contains shelly marine sediment overlain by olive brown sandy silt with an upward transition from mixed brackish and marine diatoms to fully brackish diatoms (dominated by *Cyclotella choctawhatcheeana*); this represents the transition from an intertidal zone to a lagoon or salt marsh following RSL regression (Fig. 9, Table 4, Supplemental Table 4). A twig associated with the uppermost instance of brackish diatoms dated to 9942–9531 cal. BP (UCIAMS-213799, index point: isolation basin upper transitional). The brackish silt is overlain by freshwater gyttja, the base of which dates 9695–

9139 cal. BP (UCIAMS-213798, freshwater limiting), indicating isolation from marine influence by this time.

### 3.1.6. D'boigyet lake core (DBGT#1; Kishkosh Inlet)

D'boigyet is the local Gitga'at name for a small lake that drains over a  $7.9 \pm 0.27$  m asl sill into Kishkosh Inlet. Core DBGT#1 consists of a stunning 10.75 vertical meters of sediment; the core would have continued but we reached the maximum possible depth of our equipment (Fig. 10, Table 4). A twig and a clamshell from sandy marine sediment at the base provide marine limiting information dating to 8380–8213 cal. BP (UCIAMS-206790) and 8372–8176 cal. BP (UCIAMS-206795), respectively. The similarity of the wood and shell calibrated dates suggests that our assumed  $\Delta R$  for marine reservoir correction is appropriate for the early Holocene. A twig associated with the uppermost instance of marine shell in the core dated to 4827–4619 cal. BP (UCIAMS-213797, marine limiting). The shelly deposit is overlain by brown gyttja with a steady transition from marine and brackish diatoms to a brackish/salt tolerant/freshwater diatom assemblage dominated by *Cyclotella choctawhatcheeana* and finally to a fully freshwater assemblage (Fig. 10, Supplemental Table 4). This sequence indicates lagoon conditions transitioning towards less and less marine input with RSL regression, and the eventual full isolation of the basin. Conifer needle

**Table 4**

Context information for isolation basin core samples, arranged from highest to lowest elevation.

Site and Sample Name/ Map ID (see Fig. 4)	Elevation	Litho- and biostratigraphy summary (bottom-to-top)	RSL Information	Associated Radiocarbon Dates (see Table 3)
White River Lake (WRL#2)	90 ± 0.23 m asl	Till or bedrock overlain by marine clay with shell overlain by brackish mud overlain by freshwater gyttja (Fig. 5).	RSL was higher than 90 m asl at 14,512–14,028 cal. BP (marine conditions), and RSL was lower than 90 m asl by 14,115–13,484 cal. BP (freshwater conditions).	UCIAMS-230961 UCIAMS-216105 UCIAMS-216113 UCIAMS-213801 UCIAMS-201809 UCIAMS-210408
Xaa Usta'a Pond (XUP#4)	67 ± 0.61 m asl	Silty clay overlain by organic-rich silt overlain by sandy silty peat. Freshwater diatoms throughout (Fig. 6).	RSL was below 67 m asl by before 13,306–12,771 cal. BP.	UCIAMS-213801 UCIAMS-201809 UCIAMS-210408
Kishkosh Bog- Pond (KBP#3)	21.9 ± 0.57 m asl	Gray sand (intertidal or marine) overlain by brackish sandy peat overlain by freshwater peat (Fig. 7).	RSL was below (but close to) 21.9 m asl by 10,152–9743 cal. BP (brackish or salt-tolerant diatom species). Sample location was near the upper intertidal zone at this time.	UCIAMS-201808
Kitkiata Lake (KITL#3)	21.5 ± 0.23 m asl	Marine sand with shell overlain by clay with dark organic-rich laminations (with very rare diatoms) overlain by brackish mud overlain by organic rich silt with salt tolerant diatoms overlain by freshwater gyttja (Fig. 8).	RSL was above 21.5 m asl at 11,811–11,376 cal. BP and 11,703–11,298 cal. BP (marine conditions) but was transitioning below 21.5 m asl at 11,591–11,245 cal. BP (brackish conditions). RSL was lower than 21.5 m asl by 11,062–10,603 cal. BP (freshwater conditions).	UCIAMS-226959 UCIAMS-226957 UCIAMS-226960 UCIAMS-226958 UCIAMS-226971
Lower Gabion Lake (LGL#2, K)	13.8 ± 0.35 m asl	Marine clay with shell overlain by marine or intertidal shelly sand overlain by brackish sandy silt overlain by freshwater gyttja (Fig. 9).	RSL was above 13.8 m asl at 10,164–9858 cal. BP (marine conditions). RSL was transitioning to freshwater (i.e. basin was a lagoon or salt marsh) at 9942–9531 cal. BP (upper end of brackish conditions). RSL was below 13.8 m asl by 9695–9139 cal. BP (freshwater conditions).	UCIAMS-213798 UCIAMS-213799 UCIAMS-163682
D'boigyet Lake (DBG#1)	7.9 ± 0.27 m asl	Marine silty sand with shell overlain by marine or intertidal silt with shell overlain by brown mud with a steady transition from marine to brackish diatoms overlain by freshwater peaty gyttja (Fig. 10).	RSL was higher than 7.9 m asl at 8372–8176 cal. BP and until 4827–4619 cal. BP (marine conditions). After this RSL was transitioning to freshwater until 3230–2892 cal. BP (i.e. basin was a lagoon or salt marsh). RSL was below 7.9 m asl by 3054–2882 cal. BP (freshwater conditions).	UCIAMS-213795 UCIAMS-213797 UCIAMS-206795 UCIAMS-206790
Kishkosh Lagoon (KL#2)	-1.35 ± 0.5 m asl	Pebbly colluvium or till overlain by sandy silty clay (provenience unknown) overlain by poorly sorted gravelly sand with wood pieces and rare marine diatoms overlain by marine sand with shell overlain by clay with marine shell overlain by organic-rich silt with some shell and a brackish-marine diatom assemblage (Fig. 11).	Complex depositional sequence – see Text and Fig. 11. RSL was likely higher than the lagoon sill for the entire postglacial period. Marine clay with shells dating to 13,307–13,054 cal. BP slumped into the lagoon from above sometime between 9091–8797 cal. BP and 1813–1631 cal. BP. RSL reached conditions similar to today (lagoon setting) by at least 1813–1631 cal. BP.	UCIAMS-230960 UCIAMS-210398 UCIAMS-213789 UCIAMS-213790 UCIAMS-210399 UCIAMS-213802 UCIAMS-201810

fragments taken from the uppermost instance of the brackish-dominated diatom assemblage dated 3230–2892 cal. BP (UCIAMS-213796, index point: isolation basin upper transitional). A conifer needle taken from just above this within fully freshwater sediment dates 3054–2882 cal. BP (UCIAMS-213795, freshwater limiting), indicating isolation from marine influence by this time.

### 3.1.7. Kishkosh Lagoon core (KL#2; Kishkosh Inlet)

Kishkosh Lagoon, located at the head of Kishkosh Inlet, has a bedrock sill  $-1.35 \pm 0.5$  m asl. This means that at low tides today the lagoon becomes completely isolated from the ocean. It also

means that if RSL ever dropped significantly below its current position the basin would have been a freshwater body of water.

Core KL#2 contains atypical stratigraphy that includes intrusive mudslide sediments, but which does not have any definitive evidence for lower RSL (Fig. 11, Table 4). At the base of the core we encountered impenetrable pebbly-cobbly sand, which we interpret as either colluvium or glacial outwash. This is overlain by sandy silty clay and 20 cm of brownish gray poorly sorted gravelly sand with pieces of wood. In this latter sediment we observed *Alnus* pollen, marine diatoms increasing in frequency from absent at the bottom to occasional in the upper portion, and a foraminifera

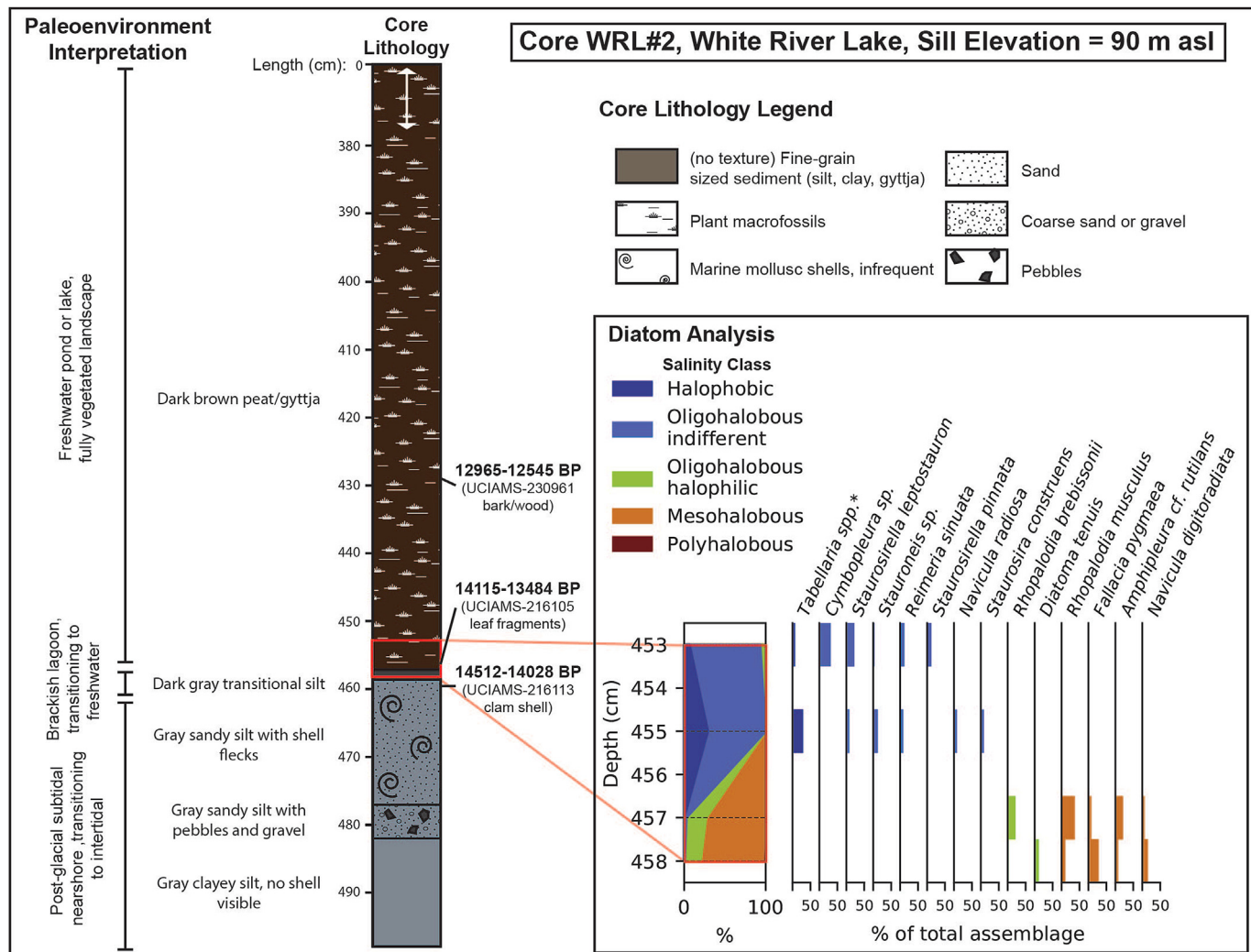


**Fig. 5.** Lower section of White River Lake core WRL#2, including core log, diatom analysis results, radiocarbon dates, and paleoenvironmental interpretations. Scale is relative to core length logged in lab. Actual field core depth = 510 cm. The 14 most common diatom species in the entire core are indicated in the expanded bar graph along with diatom summary results. \**Tabellaria* spp. = *Tabellaria flocculosa*, *T. fenestrata*, and *T. ventricosa*.

resembling a benthic *Globigerina* sp. (Supplemental Table 4). This deposit is bracketed by radiocarbon ages of 11,695–11,306 cal. BP (UCIAMS-201810) and 9535–9477 cal. BP (UCIAMS-213802). We anticipate these lowest sediments in this core to have been deposited in subtidal conditions, though they differ from subtidal deposits in other cores in our study. Typically, subtidal deposits are characterized by blue-gray, fine textured sediments, often with shell, though the coarser texture along with the wood fragments in Kishkosh Lagoon suggests nearshore deposition. However, though rare, the benthic marine diatoms and the foraminifera suggest marine deposition. Additionally, many radiocarbon ages on marine deposits in higher elevation cores indicate that RSL was higher between 11,500 and 9500 years ago.

Overlying these lowest deposits, shelly sand yielding ages of 9245–9023 cal. BP (UCIAMS-210399) and 9091–8797 cal. BP (UCIAMS-213790) indicates definite marine or intertidal conditions (Fig. 11, Table 4). Above this is a sharp transition to gray clay with shell with abundant planktonic marine diatoms: sediment typical of a deep subtidal environment, and therefore implying rising RSL since it overlies shelly sand. However, a mussel shell fragment from near to the top of the layer dated 13,307–13,054 cal. BP (UCIAMS-

213789) – much older than the multiple dated samples below it, indicating that the clay is intrusive. The most parsimonious explanation for terminal Pleistocene-aged deep-water clay to end up overlying early Holocene shelly sand is that the clay was originally deposited at a higher elevation during higher terminal Pleistocene RSL, and that it subsequently moved downwards. The clay likely represents a landslide of paleomarine sediment that slumped down the steep slopes surrounding the lagoon sometime after 9000 BP. At the upper half of the core, the clay is overlain by organic-rich silt with occasional shell, plant macrofossils, and mixed brackish and marine diatoms, consistent with a lagoon environment (Fig. 11). Wood from this lagoon silt above the clay dated 1813–1631 cal. BP (UCIAMS-210398, index point: lower lagoon) and 1550–1415 cal. BP (UCIAMS-230960, index point: lower lagoon) bracketing the potential timing of the landslide and indicating that most of the Holocene sediment is missing from this core. Overall, the dated sequence indicates subtidal or low intertidal conditions until at least 9000 BP, a landslide occurring between ~9000 and ~1700 BP, and brackish-marine lagoon conditions like that of today by at least 1700 BP.

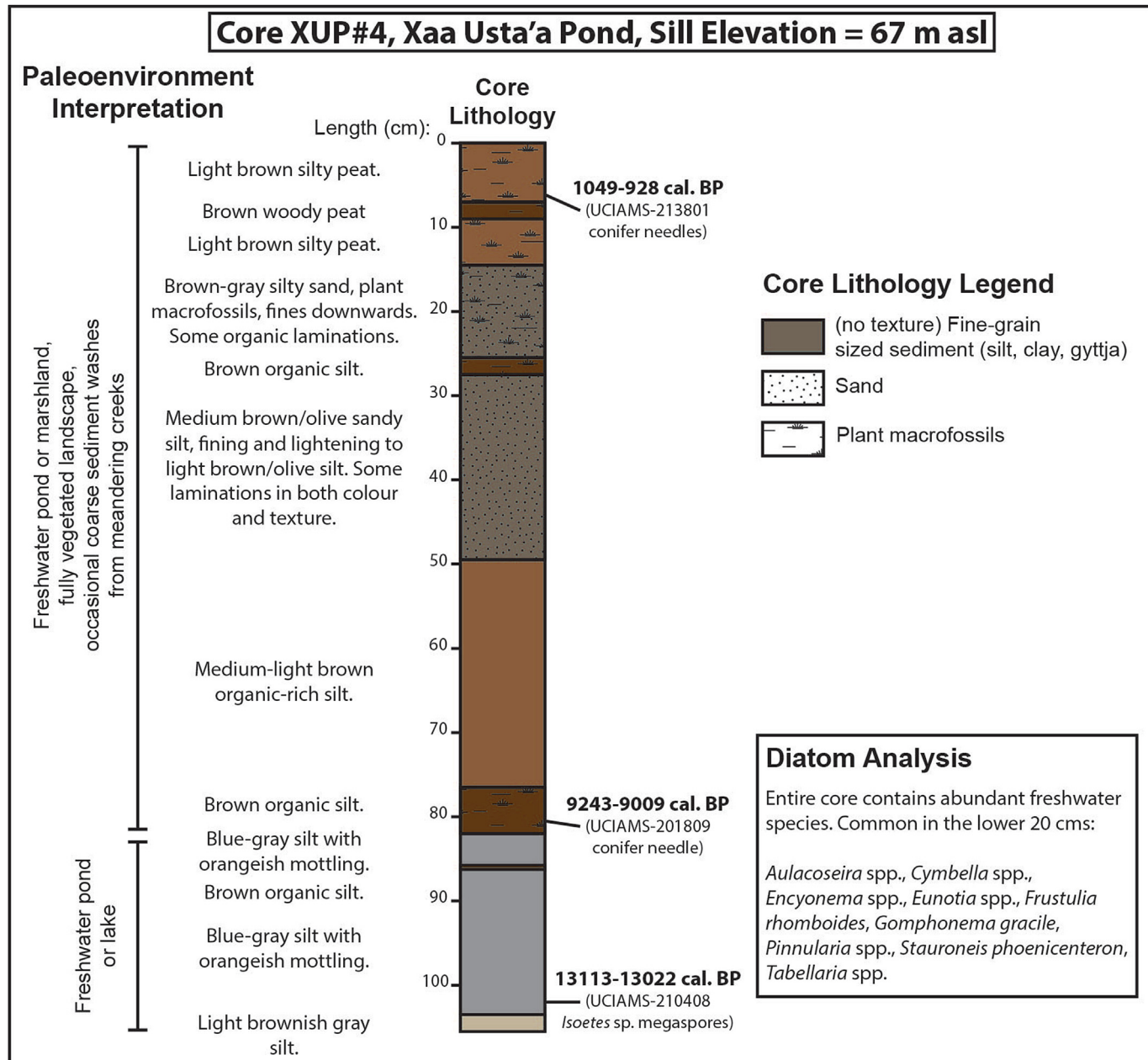


**Fig. 6.** Xaa Usta'a Pond core XUP#4, including core log, diatom analysis results, radiocarbon dates, and paleoenvironmental interpretations. Scale is relative to core length logged in lab. Actual field core depth = 114 cm. No formal diatom quantification was conducted, but the entire core contains abundant freshwater species.

### 3.2. Paleomarine exposures

Nearly all of the raised paleomarine deposits that we identified date between 13,000 and 8800 BP and indicate a general trend of falling RSL during that time (Table 3).

#### 3.2.1. Ts'm Ga Lo'op coral (Quaal/Kitkiata watershed)

Ts'm Ga Lo'op is the Gitga'at name for a sharp bend in Kitkiata River where it hits a vertical bedrock cliff (location H on Fig. 4). We identified *in situ* calcium carbonate remains of *Caryophyllum arnoldi* coral adhering to bedrock between  $5.5 \pm 0.6$  m asl down to where the bedrock meets the riverbed (~2.5 m asl). The bedrock face used to be covered in blue-gray clay but was exposed by recent slumping. A sample of the coral dated 14,750–14,145 cal. BP (UCIAMS-195676). This is the earliest age in our dataset and provides a

minimum for deglaciation of the study area. *C. arnoldi* typically lives in water depths between 40 and 656 m below sea level (Cairns, 1994), meaning that RSL was at least  $45.5 \pm 0.6$  ( $40 + 5.5 \pm 0.6$ ) m higher when this coral was alive. However, the slightly younger date on marine shell from the White River Lake core indicates that RSL was actually a minimum of 90 m asl when the coral was alive. Sometime likely between 14,500 and 14,000 years ago this bedrock cliff was covered in a slump of marine clay that preserved the calcium carbonate skeletons of the coral until its recent exposure.

#### 3.2.2. Upper Kitkiata River paleomarine exposure (Quaal/Kitkiata watershed)

This is a 15-vertical meter stratigraphic sequence exposed in the riverbank of the upper Kitkiata River that extends from 21 m asl to 36 m asl (location I on Fig. 4; Fig. 12). In this location the river has

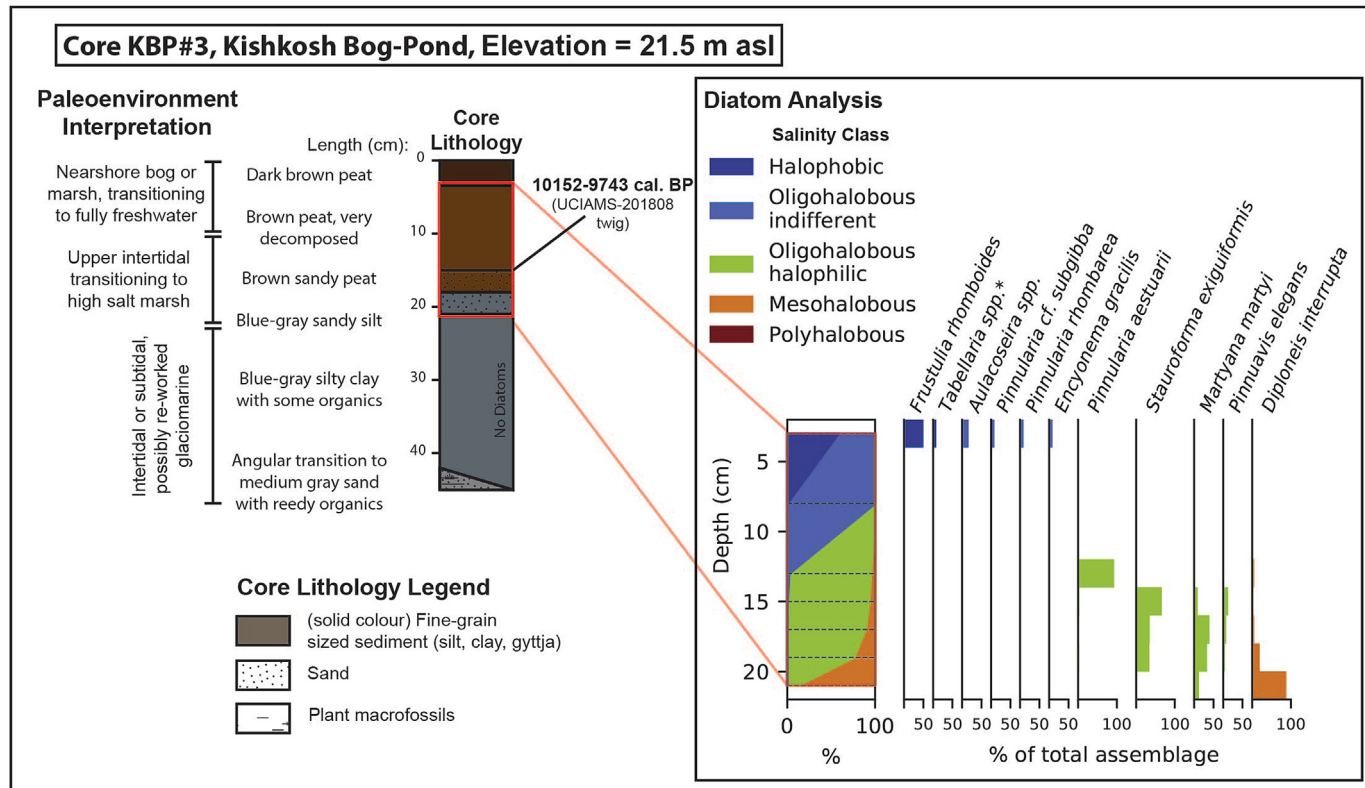


**Fig. 7.** Kishkosh Bog-Pond core KBP#3, including core log, diatom analysis results, radiocarbon dates, and paleoenvironmental interpretations. Scale is relative to core length logged in lab. Actual field core depth = 46 cm. The 11 most common diatom species in the entire core are indicated in the expanded bar graph along with diatom summary results. \**Tabellaria* spp. = *Tabellaria flocculosa*, *T. fenestrata*, and *T. ventricosa*.

cut through the potential moraine ridge that bounds the south end of Kitkiata Lake (see Kitkiata Lake core description, above). The base of the exposure consists of blue gray clay with small fragments of reworked marine shell and some pebbles from the river bed up to about  $28 \pm 1.5$  m asl. A shell from the top of this bed dated 13,051–12,745 cal. BP (UCIAMS-225534), indicating RSL at or above that elevation at this time. The shelly deposit is overlain by clay with no shell but which includes rounded pebbles that may be glacial dropstones. This deposit is in turn overlain by coarse gray sand. Above this there is a section of slope that is obscured by slumping and vegetation, but some rounded boulders sit on the surface. These may be part of a glacial till deposit overlying the paleomarine deposit. In an exposed section at the top of the riverbank slump there is more blue gray clay with rounded pebbles (Fig. 12). Above this is laminated sandy silt up to a transition to forest soil horizons; the laminations indicate deposition in water.

If the pebbles mixed in with and above the shelly zone are dropstones, they indicate deposition in an ice-proximal environment. If the boulders above are from a till deposit then they would indicate a periglacial or ice-covered environment, suggesting that the valley-perpendicular ridge at the south end of Kitkiata Lake is indeed a moraine. Given that the White River Lake core demonstrates ice-free conditions by 14,000 BP, the dropstones and till would suggest a glacial re-advance shortly after 13,000 BP – likely during the Younger Dryas (cf. Friele and Clague, 2002).

### 3.2.3. Quaal River Shell Exposures (Quaal/Kitkiata watershed)

Erosion by meanders as far as 15 km up the Quaal River has exposed numerous relict shell beds buried beneath alluvial sediment and forest soils. We dated six different exposures (Fig. 4 and Supplemental Figure 1; Table 5). The elevations of the tops of the

shell beds range from  $3.4 \pm 0.5$  m asl to  $1.7 \pm 0.8$  m asl. The oldest shell age comes from the furthest upriver exposure (Quaal River Shell Exposure, 2017–003); a *Nuculana pernula* shell from  $2.3 \pm 1.1$  m asl dated 12,481–12,048 cal. BP (UCIAMS-195677). *N. pernula* typically thrives in waters with depths of 20–1400 m (Coan et al., 2000), therefore RSL was at least  $22.3 \pm 1.1$  ( $20 + 2.3 \pm 1.1$ ) m higher than present when the specimen was alive. The ~13,000 BP freshwater conditions at 67 m asl in Xaa Usta'a Pond discussed above constrain the maximum depth of water.

Six ages from marine shell at the remaining five Quaal River exposures dated between 11,347–11,118 cal. BP (UCIAMS-180104) and 9458–9254 cal. BP (UCIAMS-163681), with the majority falling between 10,500 and 9500 BP (Supplemental Figure 1; Table 5). Five of the six ages are on growth position *S. gigantea* specimens, meaning that they minimally indicate RSL 1.4 m higher than their observed elevation (Table 2). The maximum and minimum indicative elevations from these shell beds indicate RSL higher than  $4.8 \pm 0.5$  m asl (maximum, Quaal River Shell Exposure, 2016–002) and  $3.1 \pm 0.8$  m asl (minimum, Quaal River Shell Exposure, 2016–005). Many of the deposits appear to have slumped downwards as a result of river meanders undercutting riverbanks and/or potentially a larger scale subsidence event, making ages on marine sediments useful only as minimum RSL marine limiting points. This is affirmed by data from isolation basin cores from Kitkiata Lake and Lower Gabion Lake that indicate RSL falling from 21.5 m asl to 14 m asl between 11,500 BP and 9500 BP (see Discussion).

The stratigraphy overlying the Quaal River shell beds indicates a regressing RSL and aggrading river pattern. That is, shell beds are often covered by well sorted sand deposited in an upper intertidal or estuarine environment, followed by coarser gravel and pebble clasts indicative of a high energy alluvial environment. These in

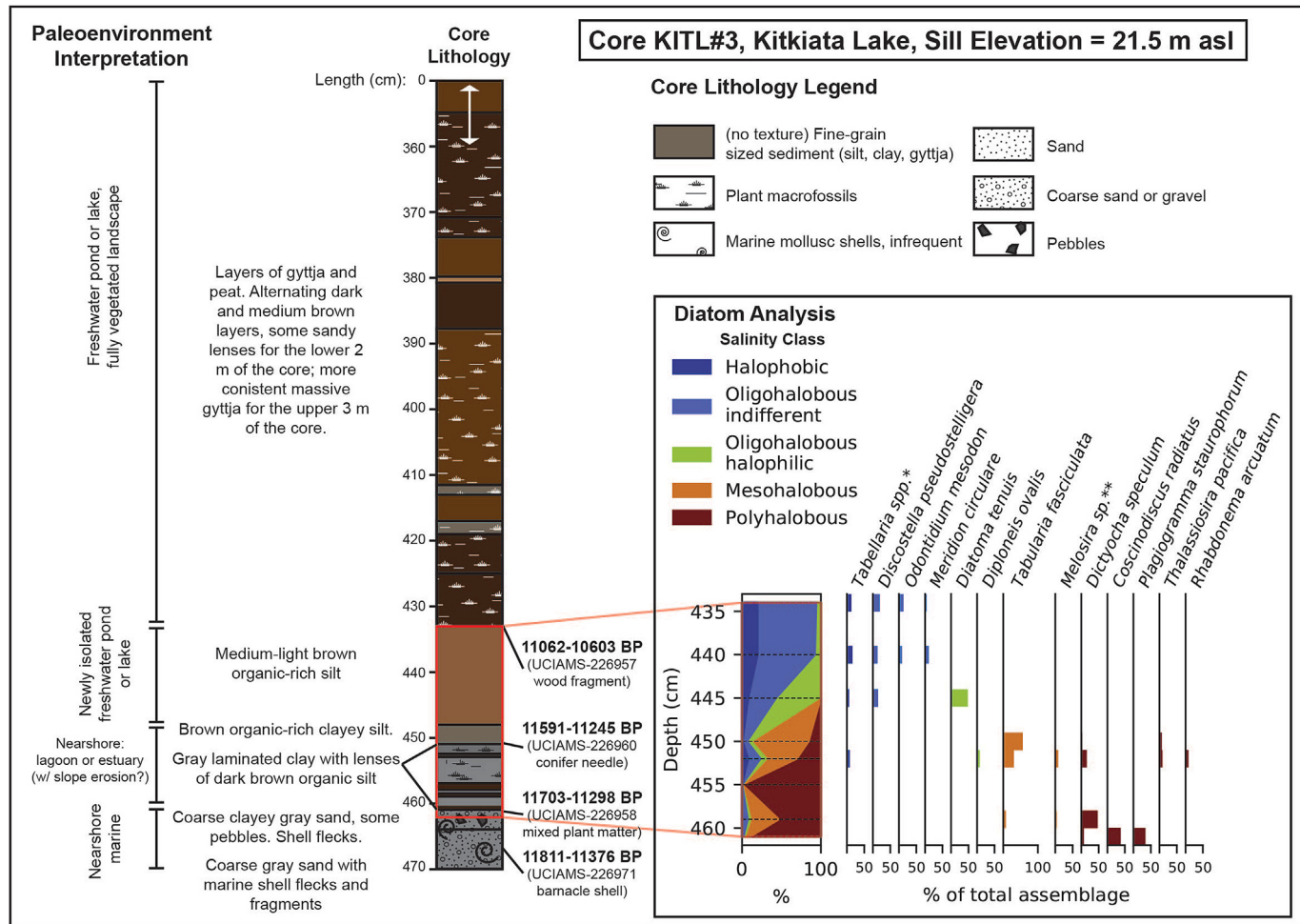


**Fig. 8.** Lower section of Kitkiata Lake core KITL#3, including core log, diatom analysis results, radiocarbon dates, and paleoenvironmental interpretations. Scale is relative to core length logged in lab. Actual field core depth = 481 cm. The 13 most common diatom species in the entire core are indicated in the expanded bar graph along with diatom summary results. \**Tabellaria* spp. = *Tabellaria flocculosa*, *T. fenestrata*, and *T. ventricosa*. \*\**Melosira* sp. = *Melosira nummuloides* or *M. moniliformis*.

turn are overlain by finer laminated organic-rich silts indicative of lower-energy alluvial deposition as the grade of the river reduced ([Supplemental Figure 1](#), [Table 5](#)). These sequences are capped by forest soils. Ages from deposits above the marine sediments provide chronological limits on falling RSL, and some indicate erosional unconformities (e.g., Quaal River Shell Exposure 206–002, see [Supplemental Figure 1](#)). However, given the likelihood that these deposits have slumped downwards, ages on freshwater/terrestrial deposits are unreliable as upper RSL elevation constraints ([Table 3](#)).

### 3.2.4. Xaa Usta'a shell exposure (Quaal/Kitkiata watershed)

Xaa Usta'a Shell Exposure is located in a small estuary flowing into Kitkiata Inlet at the mouth of the Quaal River (location G on [Fig. 4](#)); a stratigraphic section extending from 1.7 m asl down to −0.8 m asl indicates a complex depositional sequence ([Supplemental Figure 1](#), [Table 5](#)). A small growth position *S. gigantea* from the base of the exposure in clay with sparse shells suggesting subtidal conditions dated 11,028–10,705 (UCIAMS-210420), whereas growth position *S. gigantea* from higher deposits that resemble low intertidal conditions dated 9445–9320 cal. BP (UCIAMS-210419) and 9195–8925 cal. BP (UCIAMS-210418). The elevations of these latter samples indicate RSL was above  $1.4 \pm 0.2$  m asl and  $1.5 \pm 0.2$  m asl respectively, though they

are separated by a layer of flat-lying wood and clam shell valves with barnacles scars that suggest a once-exposed intertidal surface. The presence of marine molluscs characteristic of low intertidal or high subtidal environments (*S. gigantea* and *Mactromeris polynyma*) in growth position above and below this surface is considered weak evidence for a slightly rising RSL or minor subsidence (possibly only on the order of tens of centimeters) between 9500 and 9000 cal. BP (see [Table 5](#)).

The upper shell bed is overlain by a RSL regression sequence indicating a transition to an estuarine and then salt marsh environment similar to that seen elsewhere in the watershed. A cobble layer between the lower intertidal deposits and overlying salt marsh dated 680–552 cal. BP (UCIAMS- 210406, not used in final RSL plot), and the base of the salt marsh dated 674–567 cal. BP (UCIAMS- 210405, index point: salt marsh) indicating RSL similar to today by 600 BP. Additionally, these dates – which immediately overlay intertidal or subtidal silt – indicate a significant erosional unconformity dating sometime after 9000 BP.

### 3.2.5. Raised paleomarine deposits in Kitkiata Inlet (Quaal/Kitkiata watershed)

We identified several locations in the upper intertidal zone in Kitkiata Inlet where growth position *S. gigantea* shells were too high in elevation to have been alive under current sea level

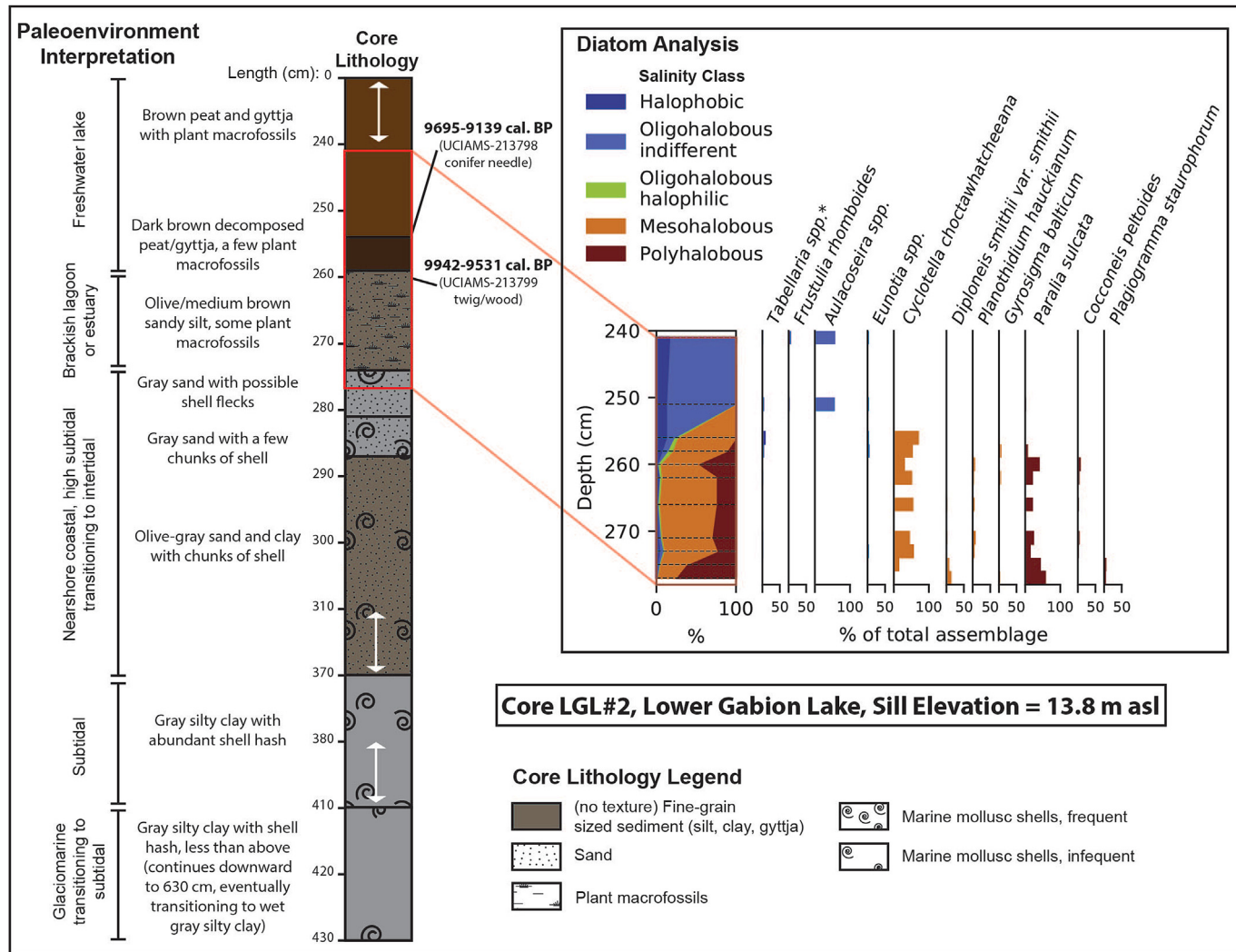


**Fig. 9.** Lower section of Lower Gabion Lake core LGL#2, including core log, diatom analysis results, radiocarbon dates, and paleoenvironmental interpretations. Scale is relative to core length logged in lab. Actual field core depth = 630 cm. The 11 most common diatom species in the entire core are indicated in the expanded bar graph along with diatom summary results. \**Tabellaria* spp. = *Tabellaria flocculosa*, *T. fenestrata*, and *T. ventricosa*.

conditions (i.e. higher than  $-1.4$  m asl). Three specimens dated 8930–8600 cal. BP (UCIAMS-210417, IST, 2018-P004), 9592–9402 cal. BP (UCIAMS-201803, IST, 2016–01), and 9572–9403 cal. BP (UCIAMS-213791, IST, 2018–08), and indicate marine limits for RSL of  $+1.1 \pm 0.2$  m,  $+1.3 \pm 0.2$  m, and  $+0.1 \pm 0.2$  m, respectively (Table 3, Supplemental Figure 1). The similarity in age but difference in elevation of the latter two samples may be because some specimens were alive below their preferred tidal range or because these samples have been subject to different post-depositional disturbances.

### 3.2.6. Malsy Creek shell exposure 2018–002 (Hartley Bay)

Malsy Creek is a small creek just south of Hartley Bay, near the mouth of Douglas Channel. There are abundant large clam shells eroding out of a sandy exposure in the creek bed  $7.15 \pm 0.8$  m asl. One of these shells dated 7561–7411 cal. BP (UCIAMS-213786, marine limiting).

### 3.3. Archaeological sites

Most of the Holocene RSL constraining data for central Douglas Channel are upper limiting dates from basal components of

archaeological sites in the Kitkiata-Quaal watersheds (22 dates from 9 sites). These sites indicate occupation as early as 8500 years ago on raised paleoshorelines, and a dropping RSL between 8500 and 2000 years ago. At two sites there is evidence for long-term occupation that followed regressing Holocene RSL: there are older archaeological components on higher elevation terraces and progressively younger ones on terraces just below these. At one site (FjTh-24, location 6 on Fig. 4), an occupation on a 13–14 m asl terrace dates between 8200 and 7500 BP (UCIAMS-206784 and UCIAMS-206785), and another on a 10–11 m surface dates 4830–4630 cal. BP (UCIAMS-206786). At Laxgalts'ap/FjTh-3 (location 7 on Fig. 4), across the mouth of Kitkiata River from the main village of the Gitga'at people at the eve of missionization in the mid-1800s, there are archaeological deposits dating at least 6500 BP (UCIAMS-206782) and potentially as early as 8500 BP (UCIAMS-206783) on a 15–17 m asl terrace. Below this, a 10–12 m asl terrace yielded dates between 3600 BP and 2800 BP (UCIAMS-210402 and UCIAMS-210403) and the lowest terrace immediately above the river has an occupation dating 1800 BP (UCIAMS-180087).

We located several other smaller sites on raised paleoshorelines without obvious continued occupations at lower elevations that support the pattern of higher RSL in the mid-Holocene. Site FjTh-25

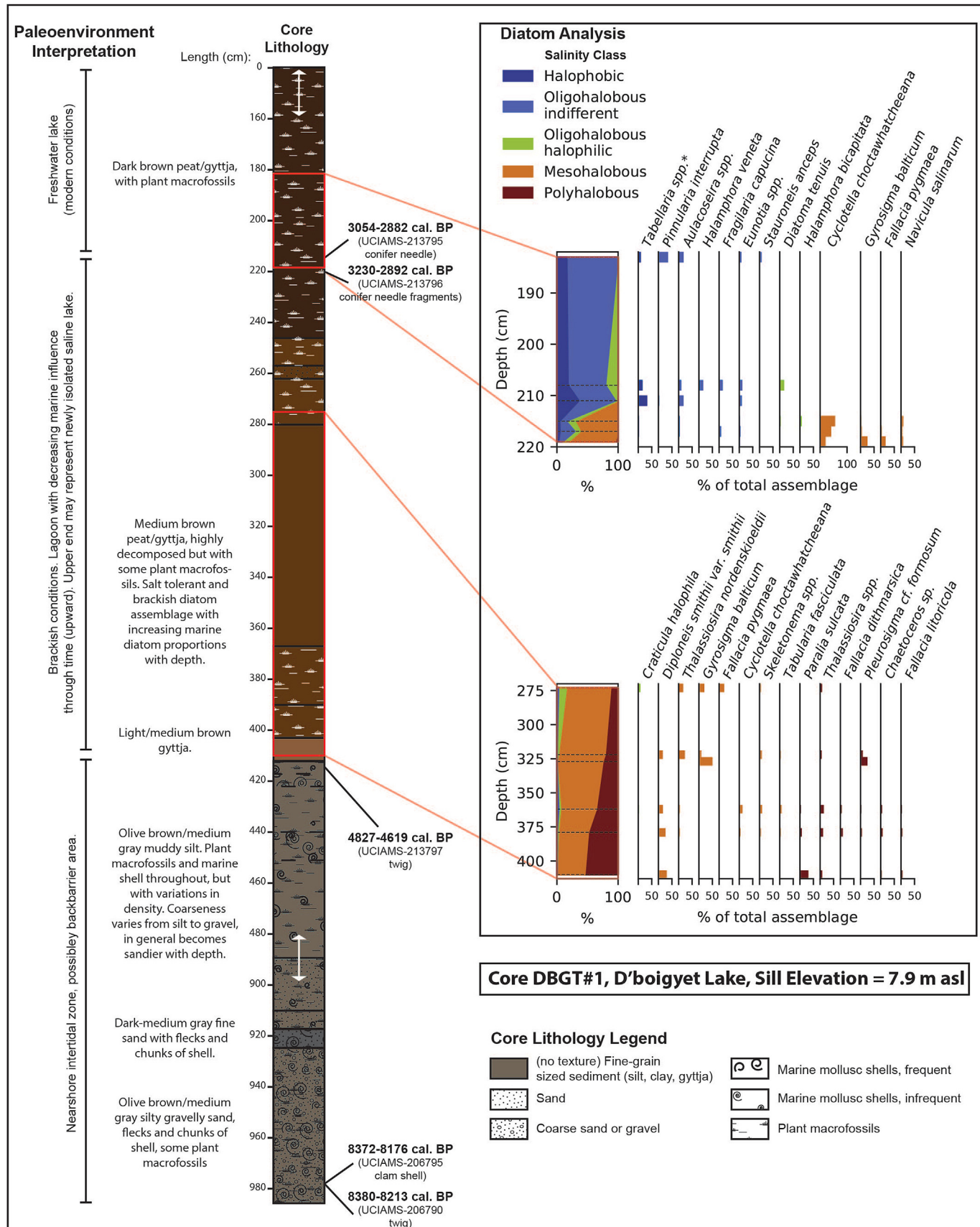


**Fig. 10.** Select sections of D'boigyet Lake core DBGT#1, including core log, diatom analysis results, radiocarbon dates, and paleoenvironmental interpretations. Scale is relative to core length logged in lab. Actual field core depth = 1075 cm. The 13 most common diatom species in two analyzed portions of the core are indicated in the expanded bar graphs along with diatom summary results. \**Tabellaria* spp. = *Tabellaria flocculosa*, *T. fenestrata*, and *T. ventricosa*.

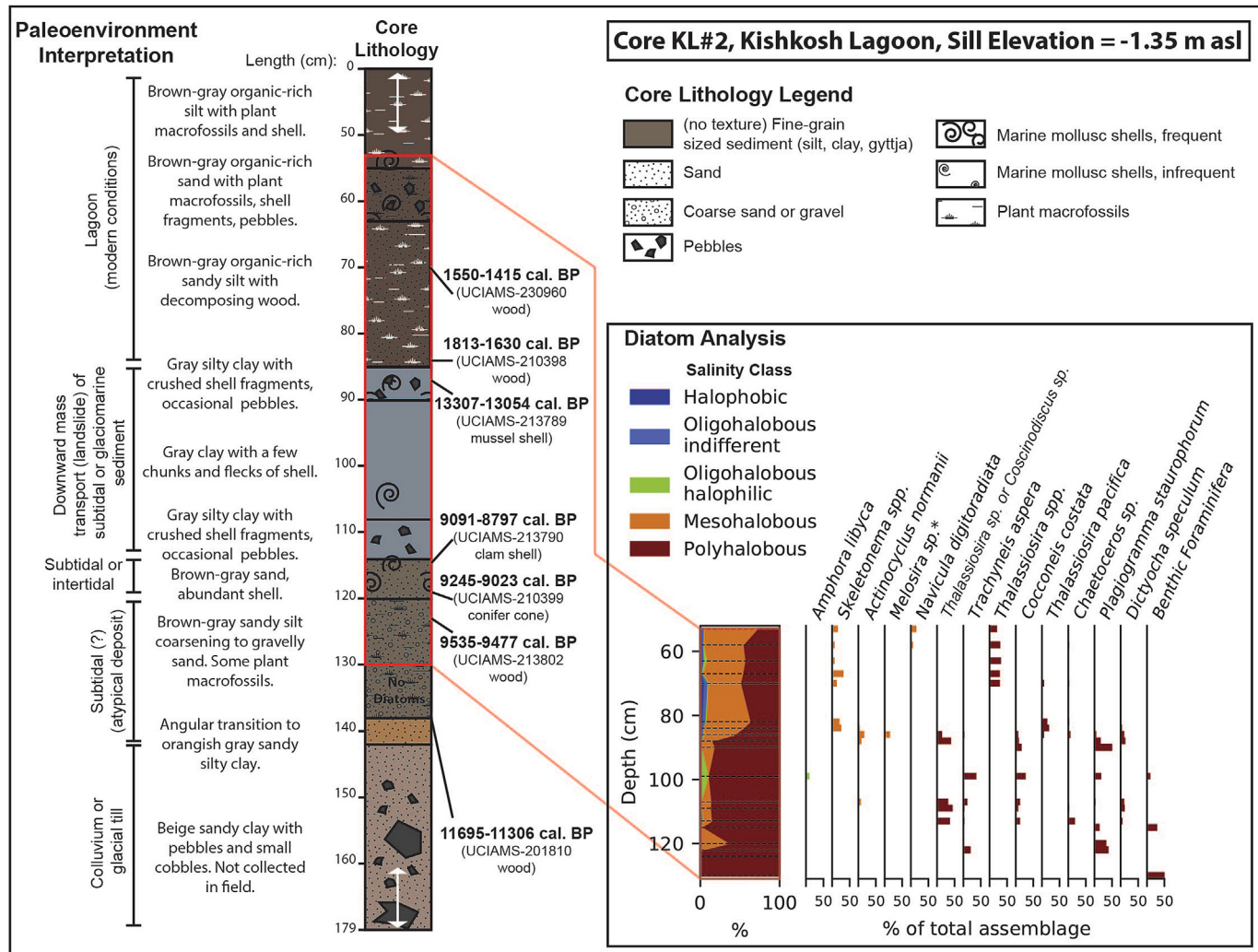


**Fig. 11.** Lower section of Kishkosh Lagoon core KL#2, including core log, diatom analysis results, radiocarbon dates, and paleoenvironmental interpretations. Scale is relative to core length logged in lab. Actual field core depth = 355 cm. The 13 most common diatom species in the entire core are indicated in the expanded bar graph along with diatom summary results. \* *Melosira* sp. = *Melosira nummuloides* or *M. moniliformis*.

dates between 5500 and 4200 BP (UCIAMS-206787, UCIAMS-206788, UCIAMS-206789) and is located on a 12–14 m asl terrace at the edge of a raised relict alluvial fan in the lower Quaal River Valley that was deposited when that area was part of the inlet (location 2 on Fig. 4). FjTh-33 is an archaeological component associated with a 7–8 m asl raised berm close to the mouth of the Quaal River that dates to 3445–3275 cal. BP (UCIAMS-210401; location 4 on Fig. 4).

Collectively, accounting for a 2.2 m HHWMT, these raised sites suggest that RSL was below 10.5 m asl from 8000 to 5500 BP, below 8 m asl around 4500 BP, and below 5 m asl by 3300 BP. All identified archaeological components associated with the present shoreline ( $n = 5$ ) date within the last 1800 years, indicating that RSL had reached close to its current position by this time.

#### 4. Discussion

##### 4.1. Central Douglas Channel RSL history and the processes driving RSL change

Taken together, our multi-proxy approach allows us to infer the RSL and deglaciation history of Douglas Channel. The age-elevation

relations of the dated samples detailed above and an inferred RSL history are shown on Fig. 13. The preserved coral at Ts'm Ga Lo'op and the marine shell in White River Lake suggest that the Quaal-Kitkiata watersheds were deglaciated by at least 14,500 BP. These earliest samples indicate that RSL was at least 90 m above its current position after deglaciation, and the wide depth range of *Carophyllia arnoldi* coral indicates that it could have been as much as 660 m higher. However, while there is evidence for RSL highstands as much as 230 m asl in the Nass River Valley (McCuaig, 2000; McCuaig and Roberts, 2006) and 170 m asl in the Kitsumkalum-Kitimat Trough (Clague 1984, 1985), there is not yet evidence in the northern Northwest Coast region for RSL any higher. Given that our data come from slightly closer to the LGM ice margin, where ice sheets would have been thinner than Nass Valley and Kitsumkalum-Kitimat Trough, we do not anticipate that RSL was so high that the *C. arnoldi* was living at the deeper end of its range.

Our oldest date on terrestrial material, from above the freshwater transition in White River Lake, indicates that the landscape was not only deglaciated but also vegetated by at least 14,115–13,484 cal. BP (UCIAMS-216105). This transition indicates emergence through isostatic uplift. Across the mainland Northwest

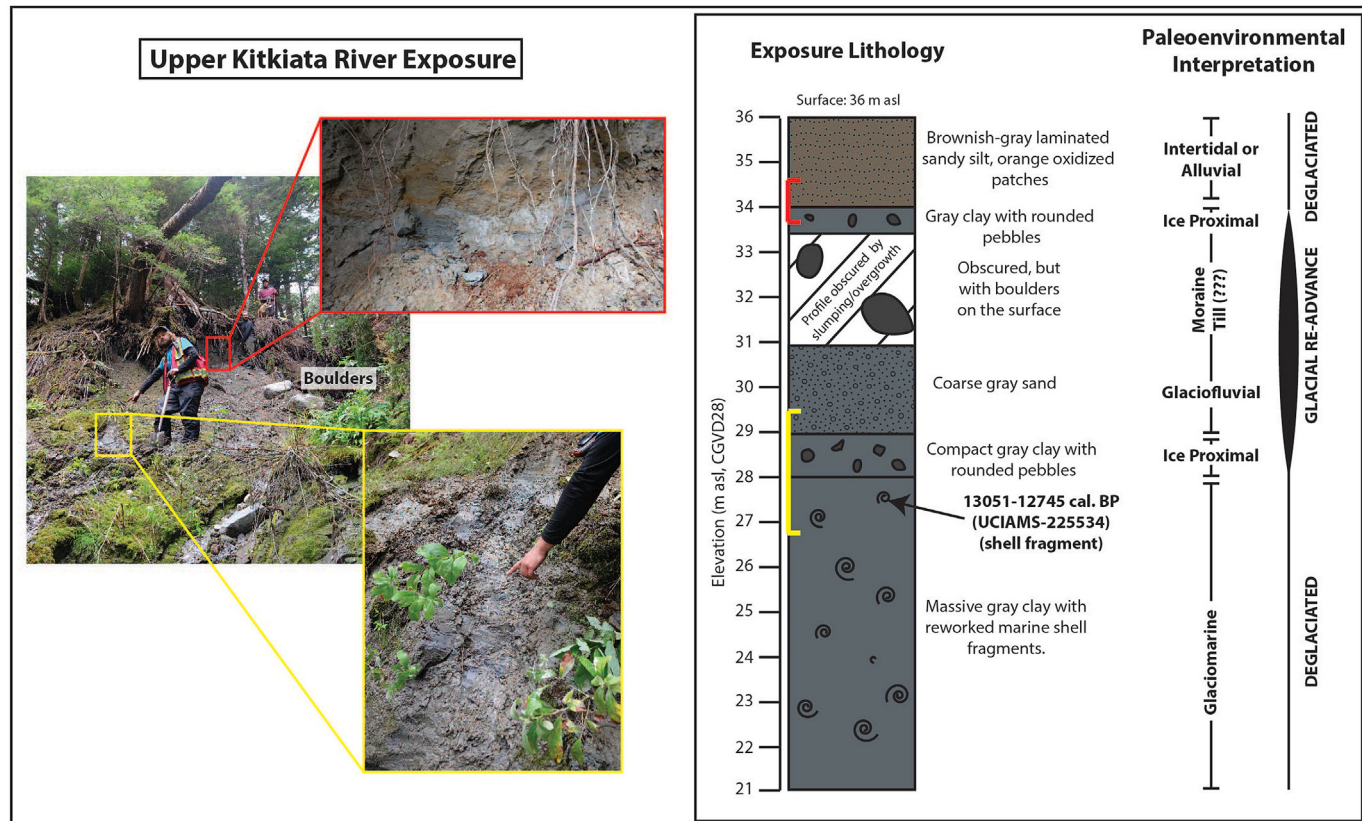


**Fig. 12.** Upper Kitkiata River Exposure, simplified stratigraphic profile, and paleoenvironmental interpretation. Sequence indicates a potential glacial re-advance after 13,051–12,745 cal. BP. Glaciomarine sediment is overlain by clay with rounded pebbles (possible dropstones in ice-proximal environment), in turn overlain by coarse sands with boulders (possible till from overriding ice), and then by clay with rounded pebbles (possible dropstones deposited by retreating/melting ice). The sequence is capped by alluvial sediment.

Coast of North America this emergence was rapid, especially at those locations most depressed by thick ice (Clague et al., 1982; Fedje et al., 2018; Letham et al., 2016; Shugar et al., 2014). A lack of accessible lakes between 90 m asl and 20 m asl in our study area means we have limited data constraining the timing or rate of this uplift, or to assess if there were potential pauses in rebound (see Fedje et al., 2018 for examples). The *Isoetes* sp. megaspores from Xaa Usta'a Pond indicate that RSL had fallen below 67 m asl by at least 13,306–12,771 cal. BP (UCIAMS-210408), while the Upper Kitkiata River Shell Exposure indicates that RSL was above  $28 \pm 1.5$  m asl at this time. The potential dropstones (pebbles in clay) and till (boulders in sand) above the dated paleomarine deposit at the latter site suggest a glacial re-advance shortly after 13,000 BP (Fig. 12); this could have caused a slowing or pause in isostatic rebound at the same time. None of our data speak directly to the exact timing or magnitude of such an effect, though a readvance likely would be associated with cooling during the Younger Dryas (cf. Friele and Clague, 2002). The Kitkiata Lake core indicates that RSL had fallen to about 20 m asl between 11,700 and 11,300 years ago and below that elevation by 11,000 years ago.

Dates on paleomarine exposures in the Quaal River Valley and the isolation basin core from Lower Gabion Lake indicate continued dropping RSL, but that the rate of isostatic rebound and resulting RSL fall had slowed significantly by as early as 11,300 BP. The Lower Gabion Lake core indicates that RSL was above 14 m asl until 10,000 BP. Following this, lower limiting constraints from marine sediment at the base of the D'boigyet Lake core and terrestrial limiting constraints from archaeological deposits at FjTh-24 indicate that RSL fell to between 8 and 11 m asl at 8200 BP. As marine limiting points,

the Quaal River shell beds support slowly falling RSL from 11,300 to 8500 BP, though the likelihood that they have dropped in elevation relative to their original position prevents us from using them as index points (see discussion in the following section). Xaa Usta'a Shell Exposure has evidence for a potential small (tens of centimeters) RSL rise between 9500 BP and 9000 BP, though our data does not provide the resolution required to resolve possible fluctuations of this scale at this time.

For the last 8000 years, isolation basin, archaeological, and exposure data indicate RSL regressing from between 8 and 11 m asl to close to its present position by 1800 BP. The D'boigyet Lake core indicates that RSL remained above about 8 m asl until 4827–4619 cal. BP (UCIAMS-213797), and paleo-high tides only fully dropped below that elevation at 3000 BP. The Malsy Creek shell exposure also indicates RSL above 8 m asl at 7500 BP. The raised archaeological components constrain the upper range of possible RSL to below 10.5 m asl and slowly dropping until 4500 BP, when it was a meter or two lower. By 3000 BP RSL had dropped to 5 m asl, and abundant archaeological sites on the modern shoreline indicate that by 1800 BP RSL had reached close to its present position.

The processes driving the slow RSL regression through the duration of the Holocene are poorly understood, though a similar pattern is evident in the Prince Rupert area (Letham et al., 2016), on the Dundas Islands (McLaren et al., 2011), and on Haida Gwaii (Clague et al., 1982; Fedje et al., 2005). On Haida Gwaii this RSL regression is attributed to slow tectonic uplift on the east side of the Queen Charlotte Fault (Fedje et al., 2005). However, compared to offshore fault zones, the northern mainland coast of British Columbia is an area of relative seismic quiescence. Therefore, the

**Table 5**

Context information for Quaal River Shell Exposures and Xaa Usta'a Shell Exposure, arranged from furthest upriver to furthest downriver. See [Supplemental Figure 1](#) for stratigraphic profiles.

Sample Site and Map ID (See Fig. 4)	Distance up-valley/ distance upriver	Highest elevation of observed shell (BOLD = RSL Indicative Meaning for growth position <i>S. gigantea</i> (elevation + 1.4 m))	Stratigraphy	RSL Information	Associated Radiocarbon Dates (see Table 3)
Quaal River Shell Exposure 2017–003 (J)	9 km/ 14.8 km	2.3 ± 1.1 m asl	<i>N. pernula</i> shells in blue-gray clayey silt exposed in riverbed.	RSL was at least 22.3 ± 1.1 m higher at 12,481 –12,048 cal. BP. ( <i>N. pernula</i> lives in water depths –20 to –1400 m asl).	UCIAMS-195677 (N. <i>pernula</i> )
Quaal River Shell Exposure 2016–004 (A)	8 km/ 12.2 km	3.3 ± 0.9 m asl (4.7 ± 0.9 m asl)	Marine shelly silt including abundant growth position <i>S. gigantea</i> shells and some cobbles with barnacle scars, overlain by well-sorted gray sand (likely upper intertidal), overlain by orange gravel (high energy alluvial), overlain by silt and clay with reedy organics (low energy alluvial).	RSL was at least 4.7 ± 0.9 m higher at 10,166 –9882 cal. BP. Some time later, RSL dropped ( <i>S. gigantea</i> ) and the area transitioned from an intertidal zone to an estuary and then a riverine environment.	UCIAMS-180101
Quaal River Shell Exposure 2016–003 (B)	7.8 km/ 11.8 km	2.6 ± 0.8 m asl (4.0 ± 0.8 m asl)	Blue-gray silt without shell (subtidal or glaciomarine) overlain by silt with abundant shell and shell hash, including growth position <i>S. gigantea</i> , overlain by well-sorted sand (upper intertidal), pebbly sand with wavy bedding (alluvial), and massive silt (low energy alluvial).	RSL was at least 4.0 ± 0.8 m higher at 10,455 –10,201 cal. BP and 10,514–10,245 cal. BP.	UCIAMS-180102 (S. <i>gigantea</i> ) UCIAMS-180105 (S. <i>gigantea</i> )
Quaal River Shell Exposure 2016–002 (C)	6.6 km/ 10.1 km	3.4 ± 0.5 m asl (4.8 ± 0.5 m asl)	Occasional growth position <i>S. gigantea</i> shells and <i>Macoma</i> sp. shells in blue gray silt, overlain by coarser gray sand (upper intertidal) followed by an irregular transition to orange-brown coarse sand and gravel with clay chunks, pieces of wood, and freshwater diatoms (high energy alluvial), overlain by laminated organic-rich silt (lower energy alluvial).	RSL was at least 4.8 ± 0.5 m higher at 11,347 –11,118 cal. BP. The area had transitioned to a freshwater environment by 3544–3380 cal. BP.	UCIAMS-180104 (conifer needle from freshwater context)
Quaal River Shell Exposure 2016–005 (D)	4.7 km/ 6.0 km	1.7 ± 0.8 m asl (3.1 ± 0.8 m asl)	Blue-gray silt with growth position <i>S. gigantea</i> and <i>Clinocardium nuttalli</i> , overlain by a meter of silt (alluvium)	RSL was at least 3.1 ± 0.8 m higher at 9686–9475 cal. BP.	UCIAMS-180103 (S. <i>gigantea</i> )
Quaal River Shell Exposure 2015–001 and 2017–001 (E)	4.1 km/ 4.7 km	2.5 ± 0.5 m asl	Blue-gray pebbly cobbley silt with a dense and diverse mollusc death assemblage, including shell hash and growth position <i>S. gigantea</i> , overlain by fine sand with shell flecks (upper intertidal), overlain by a thin mat of plant material with mixed fresh, brackish, and marine diatoms (estuarine), overlain by laminated organic-rich pebbly silt (estuarine), overlain by a massive bed of organic rich silt (alluvium).	RSL was at least 2.5 ± 0.5 m higher at 9458–9254 cal. BP. The area was an estuarine environment by 9391–9035 cal. BP and 9397–9126 cal. BP. By 1692–1558 cal. BP, forest was established on the top of the terrace at 7.75 m asl.	UCIAMS-163681 (barnacle) UCIAMS-201812 (conifer needle from estuarine sediment) UCIAMS-213804 (twig from upper estuarine sediment) UCIAMS-195668 (charcoal from upper forest)
Xaa Usta'a Shell Exposure	0 km/ 0 km	Three vertically layered beds with growth position <i>S. gigantea</i> :	Blue-gray silty clay with small, sparsely distributed shell including small growth position <i>S. gigantea</i> (low intertidal-subtidal). Coarsens upwards to well sorted gray silt with some shell and then a dense jumbled shellfish death assemblage with bivalves in growth and secondary position (low intertidal). Death assemblage is capped with a layer of flat-lying wood and clam shell valves with barnacles representing a once-exposed beach surface, then overlain by well sorted gray silt with large growth position <i>S. gigantea</i> (low intertidal; possible minor RSL rise?). Shell bed is overlain by well-sorted gray silt (estuarine), unconformable overlain by to cobbles, (high energy alluvial), overlain by silt with reedy organics (salt marsh).	RSL was above 0.7 ± 0.2 m asl at 11,015 –10,677 cal. BP (likely well above, see other data). RSL was at least 1.4 ± 0.2 m higher by 9445–9320 cal. BP and 1.5 ± 0.2 m higher by 9195–8925 cal. BP; these latter two ages are on growth position <i>S. gigantea</i> that are separated by an intertidal surface dating 9429–9299 cal. BP, together forming weakly suggestive evidence of a minor RSL rise. The area was an active river channel at 680–552 cal. BP and had transitioned to a salt marsh indicating RSL similar to today's position at 674–567 cal. BP.	UCIAMS-210420 (S. <i>gigantea</i> ) UCIAMS-210419 (shellfish death assemblage) UCIAMS-210407 (wood from buried intertidal-high subtidal surface) UCIAMS-210418 (S. <i>gigantea</i> ) UCIAMS-210406 (wood from alluvial cobbles) UCIAMS-210405 (conifer needle from base of salt marsh)

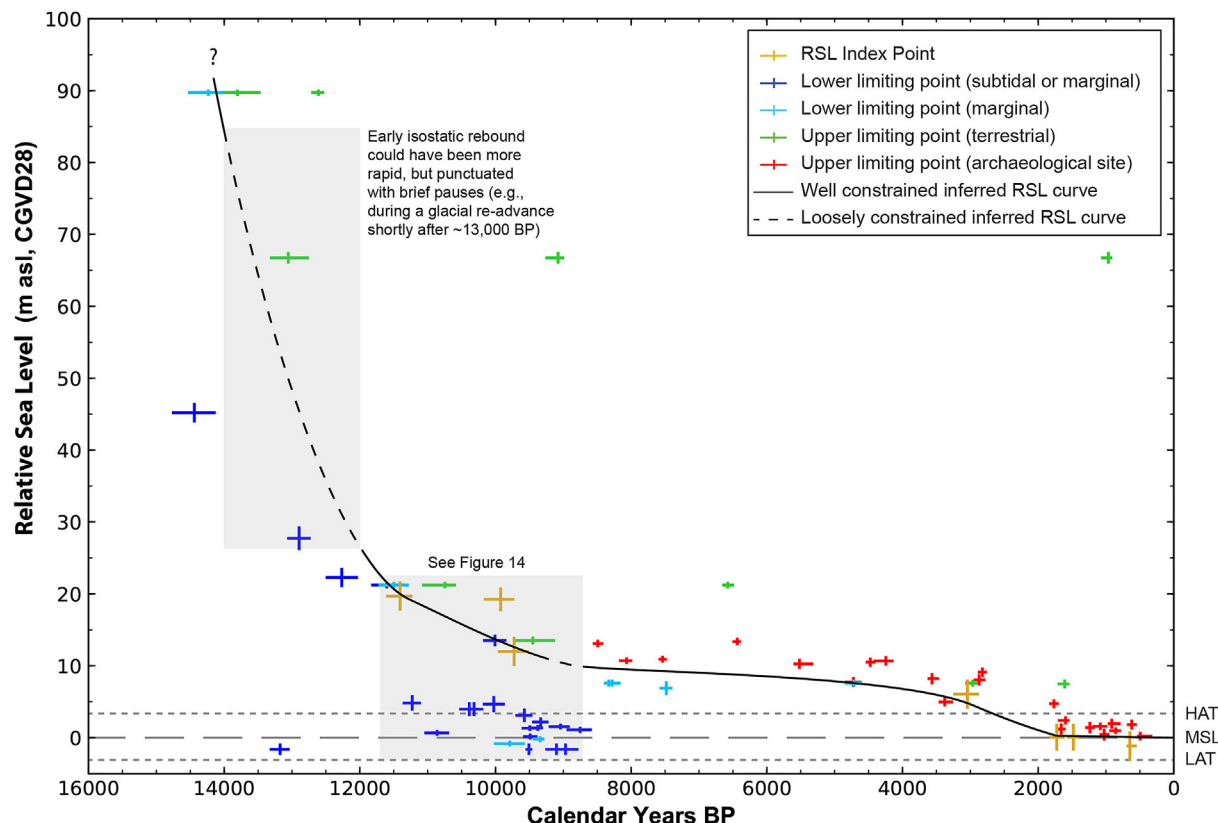


**Fig. 13.** Inferred RSL Curve for the Central Douglas Channel area based on multiple proxies. HAT = current highest astronomical tide, MSL = current mean sea level (CGVD28), LAT = current lowest astronomical tide.

apparently wide-reaching RSL fall across the mainland coast may be related to the final influence of slowing isostatic rebound in the region (T. James, personal communication 2021). Residual isostatic response might be expected on the north coast because the thick central ice dome of the Cordilleran Ice Sheet was located over the Skeena Mountains, ~250 km NNE of central Douglas Channel; the ice dome was the last part of the Ice Sheet to decay in the mid-Holocene (Seguinot et al., 2016). Therefore, isostatic uplift may have persisted longer in areas more proximal to the ice sheet center. Presently, members of the Gitga'at community are noticing increased erosion of shorelines around their ancient village sites in *Laxgalts'ap*, suggesting that anthropogenically-driven RSL rise is affecting the coastline.

#### 4.2. Evaluating the data: reconstructing RSL in dynamic landscapes

The multi-proxy approach to reconstructing RSL highlights the need for attentiveness to post-depositional geomorphic processes on RSL data. Our initial sampling design targeted growth position *S. gigantea* shells because we – and others (Carlson and Baichtal, 2015; Letham et al., 2016) – assumed that these samples could reliably be used as RSL index points because of their known relatively narrow preferred habitat elevation range around zero tide level (between LLWMT +0.5 m and LLWMT -1.0 m; Chew and Ma, 1987; Foster, 1991). However, in our dataset we found a significant discrepancy between RSL reconstructed from isolation basin cores and RSL reconstructed from *S. gigantea* shells. If we were to assume the growth position *S. gigantea* exposed in the Quaal River shell beds were index points with an indicative meaning of this narrow tidal range, then the 11 dated growth position *S. gigantea* specimens would have indicated RSL as much as 6.6 m higher than

present falling slowly to between 3 and 1 m higher between 11,300 and 8600 BP (Table 3, Fig. 14). However, the Lower Gabion Lake isolation basin indicates RSL above 14 m asl until 10,000 BP. These data indicate an elevation discrepancy of 7–10 vertical meters for RSL at 10,000 BP between two areas (Fig. 14). Lower Gabion Lake is located 25 km south from the Quaal/Kitkiata area, near the mouth of the Douglas Channel. Unfortunately, no appropriate ponds or lakes exist at 14 m asl in the Quaal/Kitkiata watershed that would allow us to test for spatial consistency with the Lower Gabion Lake result using the isolation basin coring method.

This discrepancy poses a problem. While we would anticipate isostatically-driven spatial variability from fjord mouth to fjord head in immediate postglacial times resulting from differences in thickness of ice masses and time-transgressive glacial retreat, the observed and accepted pattern is generally that RSL is higher later in time as one moves inland up the fjord (Clague et al., 1982; Clague and James, 2002). An apparently higher RSL at the mouth of Douglas Channel than in the middle of the Channel at 10,000 BP suggested by assuming *S. gigantea* are index points goes against this expectation. Because of this, and because isolation basins are more reliable RSL indicators (Table 2), parsimony required us to conclude that our growth position *S. gigantea* can only be used as marine limiting points.

This finding requires unpacking, because *S. gigantea* have been used as RSL index points in some studies, and rejected as index points in others. Relict shell beds are relatively common on the Northwest Coast, easily sampled, and do not require specialized analysis to interpret. Carlson and Baichtal (2015) rely almost exclusively on growth position *S. gigantea* to reconstruct RSL patterns in Southeast Alaska, however they have a well-sampled suite of archaeological upper limiting constraints that neatly follow the

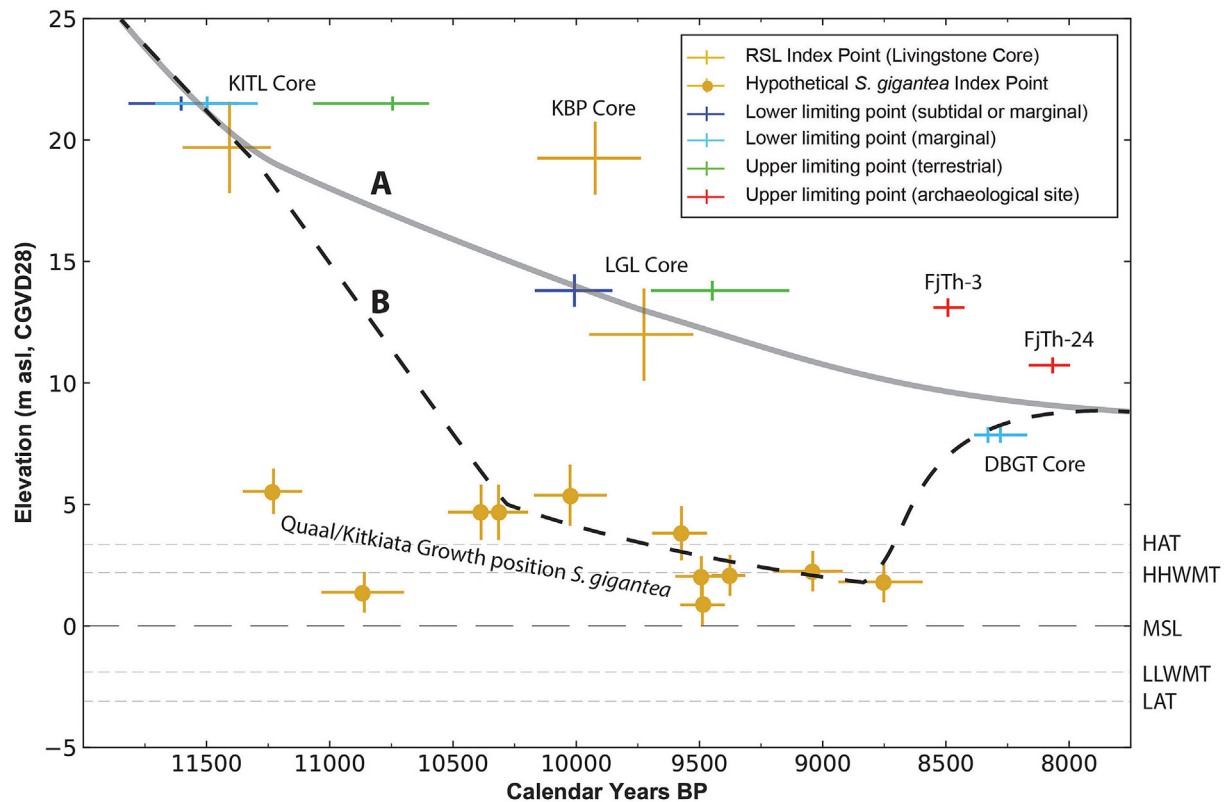


**Fig. 14.** Extract of data from Fig. 13 from 12,000 to 8000 BP with growth position *S. gigantea* hypothetically plotted as RSL index points. Note the discrepancy of 7–10 m elevation if we assume that *S. gigantea* are reliable Index Points (Line B, dashed line). The trend of RSL fall suggested by *S. gigantea* as index points is essentially parallel to the inferred RSL fall based on other data (Line A, solid gray line), suggesting consistent down-warping (slumping, tectonic subsidence, or sediment auto-compaction) of the clam shell deposits along the length of the river.

regressing raised RSL indicated by the clams. Conversely, on Haida Gwaii Fedje et al. (2011:91–96) identified a relict bed of growth position *S. gigantea* from the early Holocene that was as low as 15 m below RSL as established from isolation basin coring, and on Quadra Island Fedje et al. (2018) determined a 2 m discrepancy between RSL indicated by growth position *S. gigantea* and RSL indicated by isolation basins. Letham et al. (2016) use several growth position *S. gigantea* as index points in their reconstruction of RSL in the Prince Rupert area, but a close look at their data reveals that if they had treated these as lower limiting points instead of index points, then more outliers in their data could be accounted for by shifting an early Holocene RSL transgression back 750–1000 years (Letham et al., 2016; Fig. 13). But what could cause growth position *S. gigantea* to be reliable RSL index points in SE Alaska, but not in the central Douglas Channel region (and southern Haida Gwaii, Quadra Island, and possibly the Prince Rupert area)?

One possibility is that the *S. gigantea* that we sampled were living below their preferred tidal range. Butter clams are known to live to 10+ m below LLWMT (Quayle and Bourne, 1972:27), though their frequency drops with depth (Chew and Ma, 1987:16). However, the fact that we consistently sampled from the tops of the relict shell beds, and that most of the beds included other intertidal species and were so dense with shell to suggest they were thriving within their ideal low-tide habitat range leads us not to favour this possibility.

Instead, we propose that the utility of beds of growth position shellfish with narrow tidal ranges as RSL indicators is determined by local geological and geomorphological factors that make them more or less susceptible to post-depositional processes. RSL indicators in soft sediments and overlying massive deposits of soft

sediments (as opposed to bedrock) can be affected by compaction, slumping, and subsidence. In the Quaal River Valley, incision and meandering of the river through the paleomarine sediment draping the valley floor may have caused large slabs of mud adjacent to the river channels to drop to lower elevation. In many cases large scallop-shaped slumps immediately behind the shell exposures are visible in LiDAR DTMs. Furthermore, at multiple locations in our study (Quaal River Shell Exposure 2016–002, Xaa Usta'a Shell Exposure, Kishkosh Lagoon) radiocarbon-dated samples in close vertical succession with large age differences indicate significant erosional unconformities; millennia of geomorphological dynamism have inevitably removed strata and caused downward movement of overlying sediment. Additionally, it is possible that a single large-scale subsidence event at or after 8700 BP caused downward movement of the soft substrate sediments in the study area. Numerous studies document near-instantaneous localized subsidence caused by earthquakes across the Pacific coast (e.g. Atwater, 1987; Hutchinson and Clague, 2017; Mathewes and Clague, 1994; Rogers, 1980). Such an event could also have caused the slope failure evident in our core from Kishkosh Lagoon. Finally, fine sediments without bedrock constraints are subject to auto-compaction through time (Massey et al., 2006; see also Fedje et al., 2018:309, 313). In the present case we assume that a mixture of these three processes explains the elevation discrepancy between the shell beds that look as if they thrived in the low tide “sweet spot” for *S. gigantea* and the isolation basin cores. Because both a single large-scale subsidence event and persistent long-term compaction could create the relatively uniform downward movement apparent in Fig. 14, we are not able to distinguish between the two as causal drivers. Random localized slumping could contribute

to some of the general noise in the *S. gigantea* elevations. Testing of locations that can control for slumping (relict shell deposits removed from fluvial action), compaction (deposits without thick sediment overburden), or subsidence (deposits immediately underlain by bedrock) could tease out drivers of post-depositional altering and help determine contexts where growth position shellfish remains could be reliably used as index points.

The *S. gigantea* case serves as a cautionary tale and allows us to make a broader point around sampling for RSL data: we must carefully evaluate post-depositional movement of samples, especially in dynamic landscapes. The Quaal Valley is the epitome of such a locale. The wide and flat valley is susceptible to change through even minor changes in RSL and has been subjected to millennia of constant river meandering. It is critical that Quaternary geologists monitor the context and reliability of their sampling locations. Isolation basins with solid sediment or bedrock sills will be the most reliable if the sediment sequence has not been subjected to mixing. Limiting data such as archaeological deposits or paleomarine deposits are reliable if they are in primary context and relict upon stable landforms. Deposits on unstable landforms in highly dynamic environments need to be treated with caution, and ideally checked against another proxy.

#### 4.3. Significance for regional studies

##### 4.3.1. Spatial applicability of the central Douglas Channel sea level curve

Variability in postglacial RSL trajectories along coastlines related to the thickness and position of glacial ice along with the timing and rate of its retreat means that we need to evaluate the broader applicability of our RSL reconstruction. Most of our RSL-constraining data are from the central and southern portion of the Douglas Channel. The data from the central area encompasses the last 14,500 years and data from near the mouth of the Channel speak to the last 10,000 years. While it may be appropriate to assume that RSL position was likely similar in central and southern Douglas Channel through the Holocene after the majority of rapid isostatic rebound had occurred, other studies have demonstrated vertical variability on the order of tens of meters within tens of kilometers immediately following deglaciation (Letham et al., 2016:187–188; McLaren et al., 2014:165). This variability results from crustal tilt caused by differential loading and unloading of glaciers as they retreated inland. The submarine moraine located in the Douglas Channel just south of the mouth of Kitkiata Inlet indicates that the glacier front paused for some time between the two areas from which we collected data (Bornhold, 1983; Shaw et al., 2017); RSL position surely differed between the mouth of the Channel and Kitkiata Inlet during this pause and immediately after it. For this reason, we assume that the earliest portion of our Central Douglas Channel RSL curve does not apply to the mouth or the head of the Channel, however we suggest that the last 10,000 years of the curve is more broadly applicable, at least to the southern Douglas Channel. Further exploration and sampling of areas beyond where we sampled would test the limits of spatial applicability of the central Douglas Channel RSL curve.

The central Douglas Channel RSL curve reinforces the high spatial variability of RSL histories along the coast and fills an important gap in our understanding of this variability. Looking further afield, the central Douglas Channel RSL curve exhibits some significant differences to other RSL trajectories on the mainland margin of the Northwest Coast. This is likely a consequence of differential effects of the isostatic forebulge (i.e., ice proximity) and the timing/rate of ice retreat across the coast and up the fjords. Notably, while poorly constrained, the rate of immediate post-glacial RSL fall resulting from isostatic rebound in the central

Douglas Channel seems lower than most other mainland sites with good constraining data (see Shugar et al., 2014). Additionally, at many mainland marginal sites on the southern British Columbia Coast, and in the Prince Rupert area to the north, RSL fell to close to or below its current position at the conclusion of initial isostatic rebound and then immediately began to rise near the terminal Pleistocene/early Holocene transition (e.g. Fedje et al., 2018; Hutchinson et al., 2004a; James et al., 2009; Letham et al., 2016; Shugar et al., 2014). The central Douglas Channel RSL seems to have been 15–20 m higher between 11,000 and 10,000 years ago, and it does not seem to have ever dropped below its current position. The closest well established RSL curve to compare against is that for the Prince Rupert area, where the trajectory and timing is different: RSL had dropped extremely rapidly to below its current position by the time it was just passing below 90 m asl in central Douglas Channel, and was rising to about 6–8 m above its current position in Prince Rupert when RSL was still dropping towards 14 m asl in the Douglas Channel (Letham et al., 2016). This is surely related to different ice loads and rates of deglaciation between the two areas: Prince Rupert would have had less ice and was deglaciated earlier; the major initial isostatic rebound would have completed earlier and RSL change would have become dominated by the rapid post-glacial eustatic sea level rise (Lambeck et al., 2014). Meanwhile, the more inland Douglas Channel RSL change was still dominated by isostatic rebound, and it had more vertical rebound overall because the ice cover was thicker. Eustatic sea level rise was outpaced by the crustal rebound. Only in the early Holocene, around 9000 BP, does RSL in both the Prince Rupert and Douglas Channel areas stabilize at a similar position and slowly drop towards its modern elevation, presumably through residual isostatic rebound that outpaced the slowed Holocene eustatic sea level rise.

##### 4.3.2. Deglaciation of the northern Northwest Coast

Our data add temporal constraints to our current understanding of deglaciation of the northern Northwest Coast (Figs. 2 and 15). While Shaw et al. (2020) suggest that the Kitkiata moraine in Douglas Channel may have been a stabilized ice front at 13,800 BP (see also Bornhold, 1983; Shaw et al., 2017); the Ts'm Ga Lo'op coral and shells and plants in White River Lake indicate that the area was ice-free before then, at least as early as 14,500 BP. Deglaciation of central Douglas Channel by 14,500 BP supports the inference of ice-free conditions at the mouth of the Channel by 15,000 BP or earlier (Fig. 15B, Bornhold, 1983:107), which would be consistent with deglaciation of the Prince Rupert area (Letham et al., 2016). If the Kitkiata moraine indicates a pause of retreating glaciers, this likely occurred before 14,500 BP. If instead the moraine represents a glacial re-advance down the Channel past the mouth of Kitkiata Inlet, the ice-free Kitkiata/Quaal watershed may have become dammed at the inlet mouth (Fig. 15D). The RSL signature for such a situation would depend on how much isostatic rebound had occurred, though the duration of this configuration would likely have been brief. The dropstones and possible till deposit immediately above shell in marine clay at the Upper Kitkiata River Exposure may be evidence of such a re-advance, as these would have been deposited in an ice-proximal environment (Fig. 12). Shell from immediately below the clay with dropstones dates 13,051–12,745 cal. BP (UCIAMS-225534), which is near the onset of the Younger Dryas period of global cooling. If cooler Younger Dryas temperatures caused a re-advance of local ice sheets, it is plausible that the Kitkiata moraine was deposited during this process shortly after 13,000 years ago. Evidence for the deglaciation of Kitimat at the head of Douglas Channel ~12,500–12,000 BP indicates that a re-advance could not likely have occurred after this (Clague 1984, 1985, 1985; Clague et al., 1982). Additionally, this scenario could explain the relatively low rate of isostatic rebound between 14,500

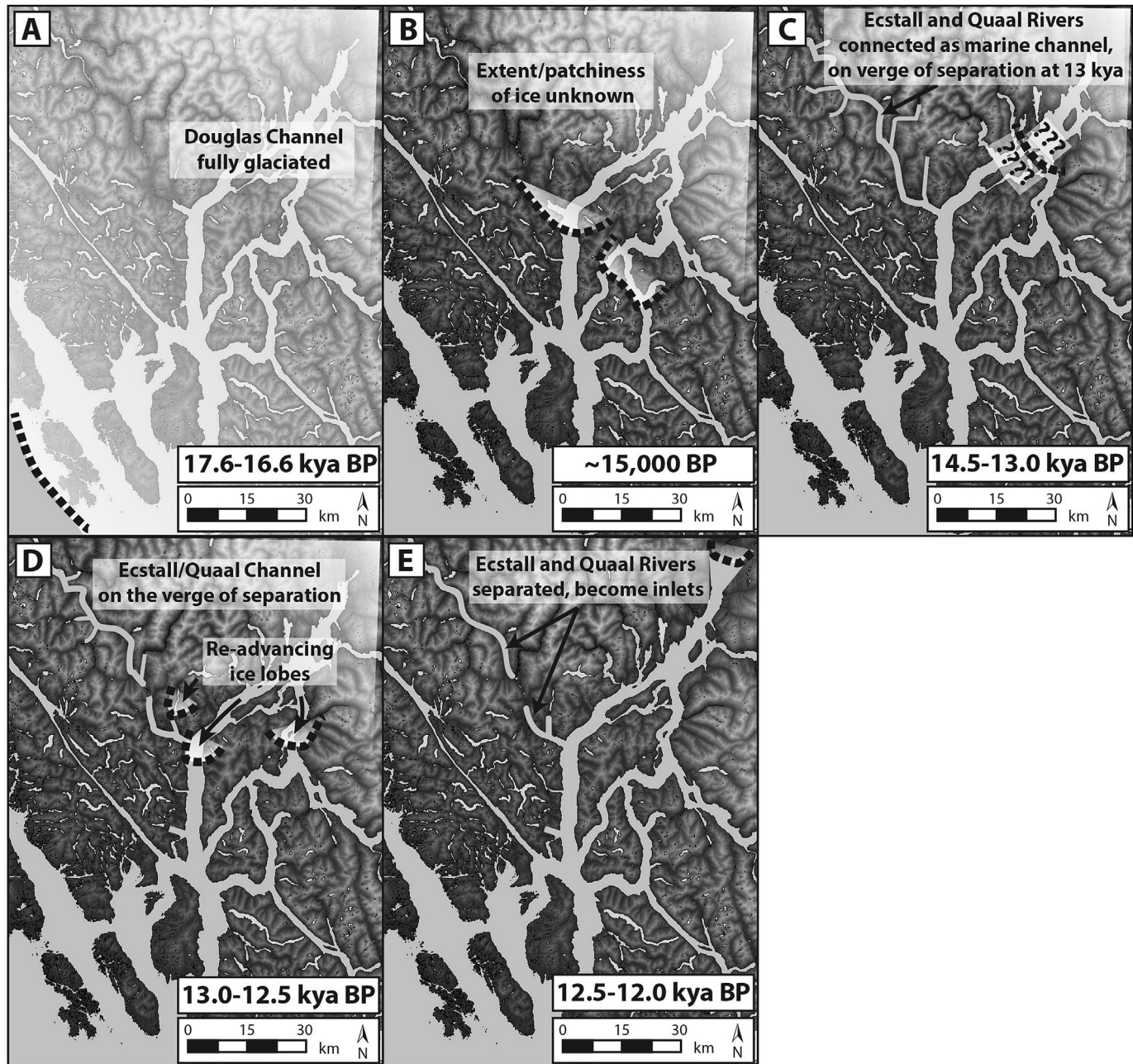


**Fig. 15.** Schematic of the history of deglaciation of the Douglas Channel area based on new results in this study and findings from Clague (1984, 1985) and Shaw et al. (2017, 2020). Dashed lines indicate ice sheet fronts. There are no data on the extent or patchiness of glaciers in the channels, fjords, and mountains beyond our immediate study area and the Douglas Channel, so these images are estimates and are incomplete. Frame D indicates a re-advance, for which we have tentative data and loose age constraints. It is the most speculative of the series. Note that this figure indicates modern shorelines on the outer islands and does not account for RSL differences at the times indicated because the RSL history of those areas is currently unknown.

BP and 12,000 BP suggested by our data: a Younger Dryas glacial re-advance could cause a pause in rebound that our poorly sampled data from this time period is not able to catch (Fig. 13, shaded area). Finally, our data do not contradict a 12,500 BP date for full deglaciation of Douglas Channel (Fig. 15E), as proposed by Clague (1984, 1985).

#### 4.3.3. Implications for early human occupation

Some of the earliest occupation of the Americas is likely to have been on the Northwest Coast (Bräje et al., 2020; Royer and Finney, 2020; Waters, 2019), so modelling where and when coastal

locations were first habitable following deglaciation is essential for searching for archaeological sites and for understanding the early postglacial environments and landscapes that initial human occupants would have lived on and moved through (McLaren et al., 2020). RSL reconstructions are key to this search, especially in areas where isostatic forces have significantly transformed the earliest shorelines. While it is likely that the outer coast was occupied before the fjords and river valleys on the mainland, people probably used the fjords and river valleys as transit corridors and moved into them soon after they became suitable for habitation. The deciduous tree leaf from central Douglas Channel

area dating to 14,115–13,484 cal. BP (UCIAMS-216105) and the shell deposits dating to slightly earlier indicate that the region supported terrestrial vegetation and edible shellfish needed for human occupation. The confirmed presence of occupation 13,500 years ago in the Calvert Island area 230 km to the south (McLaren et al., 2015; McLaren et al. 2018, 2020) indicates that people could have been in the vicinity of the lower Douglas Channel by at least that time. However, if glaciation re-advanced down the inlets and channels at the onset of the Younger Dryas period, as our data may indicate, the central Douglas Channel may have become inhospitable around then and remained so for a brief period.

Higher post-glacial RSL means that early travel corridors along the coast would have been different following deglaciation. On the isostatically-depressed mainland many of the river valleys and low passes would have been inlets and channels that may have increased interconnectivity along the coast. The pass between the Ecstall River Valley and the Quaal River Valley, which connects the Skeena River watershed to the Douglas Channel (Fig. 1B) has a maximum elevation of 60 m asl. As long as the pass was ice-free, this route would have been a marine channel connecting two fjords until about 13,000 BP, when the *Isoetes* sp. megaspores in Xaa Usta'a Pond indicate that RSL had passed below 67 m asl (Fig. 15C). With the Skeena River Valley an inlet, north-south marine travel would have been possible along the Quaal-Ecstall Channel the same way as the Grenville Channel provides passage from the mouth of the Skeena River to the mouth of the Douglas Channel today. Even after this marine channel was bifurcated by emerging land after 13,000 BP (Fig. 15E), the two sides would have been shallow and productive inlets transforming to productive estuaries at the beginning of the Holocene. By at least 11,500 years ago these zones probably would have become optimal for human occupation as indicated by the abundant early Holocene raised shellfish beds found throughout most of the ancient Quaal River Valley.

The early ancestors of the Gitga'at lineage who's *adawx* describes their settlement of Kitkiata Inlet from the north would likely have first arrived when both the Ecstall River and the Quaal River were shallow inlets. They would have settled on shorelines that are now located far up the river valley. Subsequent sedimentation through alluviation and colluviation combined with erosion through river meandering may have obscured or destroyed early archaeological remains in the valley. However, our archaeological survey has identified archaeological components >8000 years old on raised shorelines, and further predictive modelling using the RSL curve and LiDAR-derived topographic maps may be used to identify and target landforms where even older archaeological remains may still be recovered (Letham et al., 2018). There is material evidence for long-distance exchange both up and down the coast and to and from the interior by the early Holocene (Carlson, 1994); the movement of people and goods along the mainland of western North America may have been facilitated by increased navigable waterways created by higher RSL during the terminal Pleistocene and early Holocene.

## 5. Conclusion

RSL reconstructions are essential for modelling past coastal landscapes and coastline change. The central Douglas Channel RSL history provides new information on the timing and effects of deglaciation in northern coastal British Columbia, gives guidance for where to look for early archaeological evidence of human occupation in the region, and fleshes out the setting of Indigenous oral histories that chronicle events occurring in the area long ago. This is the only well-constrained sea level curve for the 350 km stretch of coast between Prince Rupert and Calvert Island/Namu, though even our extensively-sampled case has aspects that could

be addressed moving forward to refine our understanding: the nature and effect of the potential glacial re-advance ~13,000 BP, the geomorphological explanations for the discrepancy between the elevations of the growth position *S. gigantea* and the isolation basin core results, and possible small RSL fluctuations between 9500 and 8500 BP in the middle of a long history of continuously falling RSL.

The complex glacial history of the region and a comparison with patterns across the coast highlights the spatial variability of RSL trajectories and emphasizes the importance of local RSL reconstructions. Reconstruction efforts are often hindered by the remoteness of these locations (limiting sampling accessibility). Additionally, the geomorphological dynamism of coasts themselves present significant challenges to RSL reconstruction efforts, as in the case where fluvial and estuarine environments erode and shift the position of RSL indicators, or when these soft sediment landscapes are subjected to seismically induced vertical motion. A multi-proxy sampling approach that is cognizant of landscape-altering processes over the long term is essential for robust RSL reconstructions that are elements for interpreting both the unique and significant ecological and cultural histories of the region.

## Author contribution

Bryn Letham: Conceptualization, Methodology, Investigation, Formal analysis, Data curation, Visualization, Writing – original draft, Writing – review & editing. Dana Lepofsky: Supervision, Investigation, Writing – review & editing, Resources, Project administration, Funding Acquisition. Spencer Greening: Investigation, Writing – review & editing

## Declaration of competing interest

We declare no conflicts of interest in this submission to the Quaternary Science Reviews.

## Acknowledgements

We are immensely grateful to Gitga'at Nation for their partnership in this research and for allowing us to work in their beautiful territory. We are also extremely appreciative for the field assistance from Donald Reece, Justin Clifton, Isiah Dundas, Gary Robinson, Jacob Kinze Earnshaw, Rasha Elendari, Mark Wunsch, Sue Formosa, Ginevra Toniello, Alex Testani, and Jerram Ritchie. Chris Picard and the Gitga'at Oceans and Lands Department provided organizational and logistical support. Alex Testani, Megan Poland, Laura Bayes, and Rolf Mathewes provided lab assistance. We thank Derek Heathfield, Santiago Gonzalez Arriola, Keith Holmes, and Eric Peterson and Christina Munck from the Hakai Institute and Brian Menounos from UNBC for acquiring and processing LiDAR data for us. John Southon provided invaluable assistance with all of our radiocarbon dating, and Thomas J. Brown aided with radiocarbon modelling. Susan Kidwell, Ian Hutchinson, Thomas James, Lucinda Leonard, and Andrée Blais-Stevens provided useful advice along the way. Eric Letham helped produce Figs. 5–11, 13, and 14. Duncan McLaren, Daryl Fedje, and Andrew Martindale provided equipment for Livingstone coring. This project was generously funded by a SSHRC Insight Grant #435-2016-0427, a Vancouver Foundation Grant #UNR16-0666, and in-kind contributions from the Gitga'at Nation and Simon Fraser University Department of Archaeology. Letham was supported by a SSHRC Postdoctoral Fellowship during fieldwork and analysis for this project, and a MEOPAR Postdoctoral Fellowship and Banting Postdoctoral Fellowship during writing. This paper was immensely strengthened by constructive feedback from Daryl Fedje and an anonymous reviewer.

## Appendix A. Supplementary data

Supplementary data to this article can be found online at <https://doi.org/10.1016/j.quascirev.2021.106991>.

## References

- Atwater, B.F., 1987. Evidence for great Holocene earthquakes along the outer coast of Washington state. *Science* 236, 942–944.
- Barrie, J.V., Conway, K.W., Mathewes, R.W., Josenhans, H.W., Johns, M.J., 1993. Submerged late quaternary terrestrial deposits and paleoenvironments of northern Hecate Strait, British Columbia continental shelf, Canada. *Quat. Int.* 20, 123–129.
- Battarbee, R.W., 1986. Diatom analysis. In: Berglund, B.E. (Ed.), *Handbook of Holocene Palaeoecology and Palaeohydrology*. John Wiley and Sons, Chichester, UK, pp. 527–570.
- Bornhold, B.D., 1983. Sedimentation in Douglas Channel and Kitimat arm. In: Macdonald, R.W. (Ed.), *Proceeding of a Workshop on the Kitimat Marine Environment*. Canadian Technical Report of Hydrography and Ocean Sciences 18. Sidney, BC: Institute of Ocean Sciences, Department of Fisheries and Oceans, pp. 88–115.
- Braje, T.J., Erlandson, J.M., Rick, T.C., Davis, L., Dillehay, T., Fedje, D.W., Froese, D., Gusick, A., Mackie, Q., McLaren, D., Pitblado, B., Raff, J., Reeder-Myers, L., Waters, M.R., 2020. Fladmark + 40: what have we learned about a potential pacific coast peopling of the Americas? *Am. Antiq.* 85 (1), 1–21. <https://doi.org/10.1017/aqc.2019.80>.
- Bronk Ramsey, C., 2009. Bayesian analysis of radiocarbon dates. *Radiocarbon* 51 (1), 337–360.
- Cairns, S., 1994. Scleractinia of the Temperate North Pacific. *Smithsonian Contributions to Zoology*, Number 557. Smithsonian Institution Press, Washington, D.C.
- Campeau, S., Pienitz, R., Héquette, A., 1999. Diatoms from the Beaufort Sea Coast, Southern Arctic Ocean (Canada): Modern Analogues for Reconstructing Late Quaternary Environments and Relative Sea Levels. *Bibliotheca Diatomologica* No. 42. J. Cramer Inc., Berlin.
- Carlson, R.L., 1994. Trade and exchange in prehistoric British Columbia. In: Baugh, T.G., Ericson, J.E. (Eds.), *Prehistoric Exchange Systems in North America*. Springer, Boston, MA, pp. 307–361. *Interdisciplinary Contributions to Archaeology*.
- Carlson, R.J., Baichtal, J.F., 2015. A predictive model for locating early Holocene archaeological sites based on raised shell-bearing strata in Southeast Alaska, USA. *Geoarchaeology* 30 (2), 120–138. <https://doi.org/10.1002/gea.21501>.
- Chew, K.K., Ma, A.P., 1987. Species Profiles: Life Histories and Environmental Requirements of Coastal Fishes and Invertebrates (Pacific Northwest): Common Littleneck Clam. US Fish and Wildl Service Biological Reports 82. US Army Corps of Engineers, p. 22. TR EL-82-4.
- Clague, J.J., 1984. *Quaternary Geology and Geomorphology: Smithers-Terrace-Prince Rupert Area, British Columbia*. Geological Survey of Canada, Ottawa, Ontario.
- Clague, J.J., 1985. Deglaciation of the Prince Rupert-Kitimat area, British Columbia. *Can. J. Earth Sci.* 22, 256–265.
- Clague, J.J., Harper, J.R., Hebda, R.J., Howes, D.E., 1982. Late quaternary sea levels and crustal movements, coastal British Columbia. *Can. J. Earth Sci.* 19 (3), 597–618. <https://doi.org/10.1139/e82-048>.
- Clague, J.J., Mathewes, R.W., Ager, T.A., 2004. In: Madsen, D. (Ed.), *Environments of Northwestern North America before the Last Glacial Maximum*. In *Entering America: Northeast Asia And Beringia Before The Last Glacial Maximum*. University of Utah Press, Salt Lake City, pp. 63–93.
- Clague, J.J., James, T.S., 2002. History and isostatic effects of the last ice sheet in southern British Columbia. *Quat. Sci. Rev.* 21 (1–3), 71–87. [https://doi.org/10.1016/S0277-3791\(01\)00070-1](https://doi.org/10.1016/S0277-3791(01)00070-1).
- Coan, E.V., Scott, P.V., Bernard, F.R., 2000. *Bivalve Seashells of Western North America*. Santa Barbara Museum of Natural History, Santa Barbara, CA.
- Conway, K.W., Barrie, J.V., 2015. Large Submarine Slope Failures and Associated Quaternary Faults in Douglas Channel, British Columbia. Geological Survey of Canada, Current Research 2015–9. Geological Survey of Canada, Ottawa, Ontario. <https://doi.org/10.4095/297316>.
- Conway, K.W., Barrie, J.V., 2018. Large bedrock slope failures in a British Columbia, Canada fjord: first documented submarine sackungen. *Geo Mar. Lett.* 38 (3), 195–209. <https://doi.org/10.1007/s00367-018-0533-y>.
- Darvill, C.M., Menounos, B., Goehring, B.M., Lian, O.B., Caffee, M.W., 2018. Retreat of the western Cordilleran Ice Sheet margin during the last deglaciation. *Geophys. Res. Lett.* 45 (18), 9710–9720. <https://doi.org/10.1029/2018GL079419>.
- Eamer, J.B.R., Shugar, D.H., Walker, I.J., Lian, O.B., Neudorf, C.M., Telka, A.M., 2017. A glacial readvance during retreat of the Cordilleran Ice Sheet, British Columbia central coast. *Quat. Res.* 87 (3), 468–481. <https://doi.org/10.1017/qua.2017.16>.
- Edinborough, K., Martindale, A., Cook, G.T., Supernant, K., Ames, K.M., 2016. A marine reservoir effect  $\Delta R$  value for Kitandach, in Prince Rupert Harbour, British Columbia, Canada. *Radiocarbon* 58 (4), 885–891. <https://doi.org/10.1017/RDC.2016.46>.
- Engelhart, S.E., Vacchi, M., Horton, B.P., Nelson, A.R., Kopp, R.E., 2015. A sea-level database for the Pacific coast of central North America. *Quat. Sci. Rev.* 113, 78–92. <https://doi.org/10.1016/j.quascirev.2014.12.001>.
- Erlandson, J.M., Graham, M.H., Bourque, B.J., Corbett, D., Estes, J.A., Steneck, R.S., 2007. The kelp highway hypothesis: marine ecology, the coastal migration theory, and the peopling of the Americas. *J. I. Coast Archaeol.* 2 (2), 161–174. <https://doi.org/10.1080/15564890701628612>.
- Fallu, M.A., Allaire, N., Pienitz, R., 2000. Fresh Water Diatoms from Northern Quebec and Labrador (Canada). *Bibliotheca Diatomologica* No. 45. J. Cramer, Berlin.
- Fedje, D.W., Mathewes, R.W. (Eds.), 2005. *Haida Gwaii: Human History and Environment from the Time of Loon to the Time of the Iron People*. UBC Press, Vancouver.
- Fedje, D.W., McLaren, D., James, T.S., Mackie, Q., Smith, N.F., Southon, J.R., Mackie, A.P., 2018. A revised sea level history for the northern Strait of Georgia, British Columbia, Canada. *Quat. Sci. Rev.* 192, 300–316. <https://doi.org/10.1016/j.quascirev.2018.05.018>.
- Fedje, D.W., Josenhans, H., Clague, J.J., Barrie, J.V., Archer, D.J., Southon, J.R., 2005. Hecate Strait paleoshorelines. In: Fedje, D.W., Mathewes, R.W. (Eds.), *Haida Gwaii: Human History and Environment from the Time of Loon to the Time of the Iron People*. UBC Press, Vancouver, pp. 21–37.
- Fladmark, K.R., 1979. Routes: alternate migration corridors for early man in north America. *Am. Antiq.* 44, 55–69.
- Foged, N., 1981. Diatoms in Alaska. *Bibliotheca Phycologica* No. 53. J. Cramer, Berlin.
- Foster, N.R., 1991. *Intertidal Bivalves: A Guide to the Common Marine Bivalves of Alaska*. University of Alaska Press, Fairbanks.
- Friele, P.A., Clague, J.J., 2002. Younger Dryas readvance in Squamish River valley, southern coast mountains, British Columbia. *Quat. Sci. Rev.* 21, 1925–1933.
- Hein, M.F., 1990. Flora of Adak Island, Alaska: Bacillariophyceae (Diatoms). *Bibliotheca Diatomologica* No. 21. J. Cramer, Berlin.
- Hijma, M.P., Engelhart, S.E., Törnqvist, T.E., Horton, B.P., Hu, P., Hill, D.F., 2015. A protocol for a geological sea-level database. In: Shennan, I., Long, A.J., Horton, Benjamin P. (Eds.), *Handbook for Sea-Level Research*. John Wiley and Sons, West Sussex, UK, pp. 536–553.
- Hustedt, F., 1953. Die Systematik der Diatomeen in ihren Beziehungen zur Geologie und Ökologie nebst einer Revision des Halobien-Systems. *Sven. Bot. Tidskr.* 47, 509–519.
- Hutchinson, I., Clague, J.J., 2017. Were they all giants? Perspectives on late Holocene plate-boundary earthquakes at the northern end of the Cascadia Subduction Zone. *Quat. Sci. Rev.* 169, 29–49.
- Hutchinson, I., James, T.S., Clague, J.J., Barrie, J.V., Conway, K.W., 2004a. Reconstruction of late quaternary sea-level change in southwestern British Columbia from sediments in isolation basins. *Boreas* 33 (3), 183–194.
- Hutchinson, I., James, T.S., Reimer, P.J., Bornhold, B.D., Clague, J.J., 2004b. Marine and limnic radiocarbon reservoir corrections for studies of late- and postglacial environments in Georgia Basin and Puget Lowland, British Columbia, Canada and Washington, USA. *Quat. Res.* 61 (2), 193–203. <https://doi.org/10.1016/j.yqres.2003.10.004>.
- James, T.S., Gowar, E.G., Hutchinson, I., Clague, J.J., Barrie, J.V., Conway, K.W., 2009. Sea-level change and paleogeographic reconstructions, southern Vancouver Island, British Columbia, Canada. *Quat. Sci. Rev.* 28, 1200–1216.
- James, T.S., Hutchinson, I., Barrie, J.V., Conway, K.W., Mathews, D., 2005. Relative sea-level change in the northern strait of Georgia, British Columbia. *Géogr. Phys. Quaternaire* 59 (2–3), 113–127. <https://doi.org/10.7202/014750ar>.
- Khan, N.S., Horton, B.P., Engelhart, S., Rovere, A., Vacchi, M., Ashe, E.L., Törnqvist, T.E., Dutton, A., Hijma, M.P., Shennan, I., the HOLSEA Working Group, 2019. Inception of a global atlas of sea levels since the last glacial maximum. *Quat. Sci. Rev.* 220, 359–371.
- Kjemerud, A., 1981. Diatom changes in sediments of basins possessing marine/lacustrine transitions in Frosa, Nord-Troendelag, Norway. *Boreas* 10 (1), 27–38. <https://doi.org/10.1111/j.1502-3885.1981.tb00466.x>.
- Kolbe, R.W., 1927. Zur Ökologie, Morphologie und Systematik der Brackwasser-Diatomeen. *Pflanzenforschung* 7, 1–146.
- Kolbe, R.W., 1932. Grundlinien einer allgemeinen Ökologie der Diatomeen. *Ergeb. Biol.* 8, 221–348.
- Krammer, K., Lange-Bertalot, H., 1986a. Bacillariophyceae 1. Teil: naviculaceae. In: Ettl, H., Gerloff, J., Heyning, H., Mollenhauer, D., Band (Eds.), *Süßwasser flora von Mitteleuropa*, 2/1. Gustav Fischer Verlag, Stuttgart, Germany, p. 876.
- Krammer, K., Lange-Bertalot, H., 1986b. Bacillariophyceae 2. Teil: bacillariaceae, epithemiacae, surirellaceae. In: Ettl, H., Gerloff, J., Heyning, H., Mollenhauer, D., Band (Eds.), *Süßwasser flora von Mitteleuropa*, 2/2. Gustav Fischer Verlag, Stuttgart, Germany, p. 596.
- Krammer, K., Lange-Bertalot, H., 1986c. Bacillariophyceae 3. Teil: centrales, fragilariaeae, eunotiaceae. In: Ettl, H., Gerloff, J., Heyning, H., Mollenhauer, D., Band (Eds.), *Süßwasser flora von Mitteleuropa*, 2/3. Gustav Fischer Verlag, Stuttgart, Germany, p. 598.
- Krammer, K., Lange-Bertalot, H., 1986d. Bacillariophyceae 4. Teil: achnanthaceae, Kritische Ergänzungen zu Achnanthes s.l., Navicula s. str., Gomphonema. In: Ettl, H., Gärtner, G., Gerloff, J., Heyning, H., Mollenhauer, D., Band (Eds.), *Süßwasser flora von Mitteleuropa*, 2/4. Gustav Fischer Verlag, Stuttgart, Germany, p. 468.
- Lambeck, K., Rouby, H., Purcell, A., Sun, Y., Cambridge, M., 2014. Sea level and global ice volumes from the Last Glacial Maximum to the Holocene. *Proc. Natl. Acad. Sci. Unit. States Am.* 111 (43), 15296–15303.
- Laws, R.A., 1988. Diatoms (bacillariophyceae) from surface sediments in the San Francisco Bay estuary. *Proc. Calif. Acad. Sci.* 45, 133–254.
- Lepofsky, D., Armstrong, C.G., Greening, S., Jackley, J., Carpenter, J., Guernsey, B., Mathews, D., Turner, N.J., 2017. Historical ecology of cultural keystone places of the Northwest Coast: historical ecology of cultural keystone places. *Am.*

- Anthropol. 119 (3), 448–463. <https://doi.org/10.1111/aman.12893>.
- Lesnek, A.J., Briner, J.P., Baichtal, J.F., Lyles, A.S., 2020. New constraints on the last deglaciation of the Cordilleran Ice Sheet in coastal southeast Alaska. Quat. Res. <https://doi.org/10.1017/qua.2020.32>.
- Lesnek, A.J., Briner, J.P., Lindqvist, C., Baichtal, J.F., Heaton, T.H., 2018. Deglaciation of the Pacific coastal corridor directly preceded the human colonization of the Americas. *Science Advances* 4 (5). <https://doi.org/10.1126/sciadv.aar5040>.
- Letham, B., Martindale, A., Macdonald, R., Guiry, E., Jones, J., Ames, K.M., 2016. Postglacial relative sea-level history of the Prince Rupert area, British Columbia, Canada. *Quat. Sci. Rev.* 153, 156–191. <https://doi.org/10.1016/j.quascirev.2016.10.004>.
- Letham, B., Martindale, A., Waber, N., M Ames, K., 2018. Archaeological survey of dynamic coastal landscapes and paleoshorelines: locating early Holocene sites in the Prince Rupert Harbour area, British Columbia, Canada. *J. Field Archaeol.* 43 (3), 181–199. <https://doi.org/10.1080/00934690.2018.1441575>.
- Long, A.J., Woodroffe, S.A., Roberts, D.H., Dawson, S., 2011. Isolation basins, sea-level changes and the Holocene history of the Greenland ice sheet. *Quat. Sci. Rev.* 30, 3748–3768.
- Proceeding of a workshop on the Kitimat marine environment. In: MacDonald, R.W. (Ed.), 1983. Canadian Technical Report of Hydrography and Ocean Sciences, vol. 18. Institute of Ocean Sciences, Department of Fisheries and Oceans, Sidney, BC.
- Mackie, Q., Fedje, D.W., McLaren, D., 2018. Archaeology and sea level change on the British Columbia coast. *Can. J. Archaeol.* 42, 74–91.
- Marsden, S., 2012. The Gitk'aata, Their History, and Their Territories. Unpublished Report prepared for the Gitga'at First Nation.
- Martindale, A., Cook, G.T., McKechnie, I., Edinborough, K., Hutchinson, I., Eldridge, M., Supernant, K., Ames, K.M., 2018. Estimating marine reservoir effects in archaeological chronologies: comparing ΔR calculations in Prince Rupert Harbour, British Columbia, Canada. *Am. Antiquity* 83 (4), 659–680. <https://doi.org/10.1017/aaq.2018.47>.
- Marty, J., Myrbo, A., 2014. Radiocarbon dating susceptibility of aquatic plant macrofossils. *J. Paleolimnol.* 52 (4), 435–443.
- Massey, A.C., Paul, M.A., Gehrels, W.R., Charman, D.J., 2006. Autocompaction in Holocene coastal back-barrier sediments from southern Devon, southwest England. *Mar. Geol.* 226, 225–241.
- Mathewes, R.W., Clague, J.J., 1994. Detection of large prehistoric earthquakes in the Pacific Northwest by microfossil analysis. *Science* 264 (5159), 688–691.
- Mathewes, R.W., Clague, J.J., 2017. Paleoecology and ice limits of the early Fraser Glaciation (Marine Isotope Stage 2) on Haida Gwaii, British Columbia, Canada. *Quat. Res.* 88 (2), 277–292. <https://doi.org/10.1017/qua.2017.36>.
- McCuaig, S.J., 2000. Glacial History of the Nass River Region. Unpublished PhD Dissertation. Simon Fraser University, Burnaby, British Columbia.
- McCuaig, S.J., Roberts, M.C., 2006. Nass River on the move: radar facies analysis of glaciofluvial sedimentation and its response to sea-level change in northwestern British Columbia. *Can. J. Earth Sci.* 43 (11), 1733–1746. <https://doi.org/10.1139/e06-073>.
- McLaren, D., Fedje, D.W., Dyck, A., Mackie, Q., Gauvreau, A., Cohen, J., 2018. Terminal Pleistocene epoch human footprints from the Pacific coast of Canada. *PLoS One* 13 (3), e0193522. <https://doi.org/10.1371/journal.pone.0193522>.
- McLaren, D., Fedje, D.W., Hay, M.B., Mackie, Q., Walker, I.J., Shugar, D.H., Eamer, J.B.R., Lian, O.B., Neudorf, C., 2014. A post-glacial sea level hinge on the central Pacific coast of Canada. *Quat. Sci. Rev.* 97, 148–169. <https://doi.org/10.1016/j.quascirev.2014.05.023>.
- McLaren, D., Fedje, D.W., Mackie, Q., Davis, L.G., Erlandson, J., Gauvreau, A., Vogelaar, C., 2020. Late Pleistocene archaeological discovery models on the Pacific coast of North America. *PaleoAmerica* 6 (1), 43–63. <https://doi.org/10.1080/20555563.2019.1670512>.
- McLaren, D., Gitla, (E. White), Rahemtulla, F., Fedje, D.W., 2015. Prerogatives, sea level, and the strength of persistent places: archaeological evidence for long-term occupation of the central coast of British Columbia. *BC Studies* 187, 155–306.
- McLaren, D., Martindale, A., Fedje, D.W., Mackie, Q., 2011. Relict shorelines and shell middens of the Dundas island Archipelago. *Can. J. Archaeol.* 35 (1), 86–116.
- Pienitz, R., Fedje, D.W., Poulin, M., 2003. Marine and Non-Marine Diatoms from the Haida Gwaii Archipelago and Surrounding Coasts, Northeastern Pacific, Canada. *Bibliotheca Diatomologica*, vol. 48. J. Cramer Inc, Berlin.
- Rao, V.N.R., Lewin, J., 1976. Benthic Marine Diatom Flora of False Bay, San Juan Island, Washington. In: Benthic Marine Diatom Flora of False Bay, vol. 9. Syesis, pp. 173–213. Syesis.
- Roe, H.M., Doherty, C.T., Patterson, R.T., Milne, G.A., 2013. Isolation basin records of late Quaternary sea-level change, central mainland British Columbia, Canada. *Quat. Int.* 310, 181–198. <https://doi.org/10.1016/j.quaint.2013.01.026>.
- Rogers, C.G., 1980. A documentation of soil failure during the British Columbia earthquake of July 23, 1946. *Can. Geotech. J.* 17, 122–127.
- Royer, T., Finney, B., 2020. An oceanographic perspective on early human migrations to the Americas. *Oceanography* 33 (1). <https://doi.org/10.5670/oceanog.2020.102>.
- Seguinot, J., Rogozhina, I., Stroeven, A.P., Margold, M., Klemen, J., 2016. Numerical simulations of the Cordilleran Ice Sheet through the Last Glacial Cycle. *Cryosphere* 10, 639–664.
- Shaw, J., Barrie, J.V., Conway, K.W., Lintern, D.G., Kung, R., 2020. Glaciation of the northern British Columbia continental shelf: the geomorphic evidence derived from multibeam bathymetric data. *Boreas* 49 (1), 17–37. <https://doi.org/10.1111/bor.12411>.
- Shaw, J., Stacey, C.D., Wu, Y., Lintern, D.G., 2017. Anatomy of the Kitimat fjord system, British Columbia. *Geomorphology* 293, 108–129. <https://doi.org/10.1016/j.geomorph.2017.04.043>.
- Shennan, I., 2015. Handbook of sea-level research: framing research questions. In: Shennan, I., Long, A.J., Horton, B.P. (Eds.), *Handbook of Sea-Level Research*. John Wiley and Sons, West Sussex, UK, pp. 3–25.
- Shennan, I., Innes, J.B., Long, A.J., 1994. Late Devensian and Holocene Relative sea-level changes at Loch Nan Eala, near Arisaig, northwest Scotland. *J. Quat. Sci.* 9 (3), 261–283.
- Shennan, I., Long, A.J., Horton, B.P. (Eds.), 2015. *Handbook of Sea-Level Research*. John Wiley and Sons, West Sussex, UK.
- Shugar, D.H., Walker, I.J., Lian, O.B., Eamer, J.B.R., Neudorf, C., McLaren, D., Fedje, D.W., 2014. Post-glacial sea-level change along the Pacific coast of North America. *Quat. Sci. Rev.* 97, 170–192. <https://doi.org/10.1016/j.quascirev.2014.05.022>.
- Törnqvist, T.E., Rosenheim, B.E., Hu, P., Fernandez, A.B., 2015. Radiocarbon dating and calibration. In: Shennan, I., Long, A.J., Horton, B.P. (Eds.), *Handbook of Sea-Level Research*. John Wiley and Sons, West Sussex, UK, pp. 349–360.
- Tynni, R., 1986. Observations of Diatoms on the Coast of the State of Washington. *Geological Survey of Finland Report of Investigations*, vol. 75. Finland, Espoo.
- van de Plassche, O., 1986. Introduction. In: van de Plassche, O. (Ed.), *Sea-level Research: A Manual for the Collection and Evaluation of Data*, vols. 1–26. Geo Books, Norwich, UK.
- Warner, B.G., Clague, J.J., Mathewes, R.W., 1982. Ice-free conditions on the queen Charlotte islands, British Columbia, at the height of late Wisconsin glaciation. *Science* 218, 676–677.
- Waters, M.R., 2019. Late Pleistocene exploration and settlement of the Americas by modern humans. *Science* 365 (6449), eaat5447. <https://doi.org/10.1126/science.aat5447>.
- Witkowski, A., Lange-Bertalot, H., Metzeltin, D., 2000. *Diatom Flora of Marine Coasts I. Iconographia Diatomologica: Annotated Diatom Micrographs*, vol. 7. A.R.G. Gantner, Königstein, Germany.
- Wright, H.E., 1967. A square-rod piston sampler for lake sediments. *J. Sediment. Res.* 37 (3), 975–976. <https://doi.org/10.1306/74D71807-2B21-11D7-8648000102C1865D>.
- Zong, Y., Sawai, Y., 2015. Diatoms. In: Shennan, I., Long, A.J., Horton, B.P. (Eds.), *Handbook of Sea-Level Research*. John Wiley and Sons, West Sussex, UK, pp. 233–248.